American Mineralogist, Volume 68, pages 667–686, 1983

High-grade metamorphism in the Chapleau-Foleyet Area, Ontario

JOHN A. PERCIVAL

Geological Survey of Canada
588 Booth Street, Ottawa, Ontario K1A 0E4 Canada

Abstract

High-grade Archean rocks are exposed in the central Superior Province of the Canadian Shield in the Kapuskasing Structural Zone, a partly fault-bounded region up to 50 × 500 km. In migmatitic mafic gneiss, paragneiss, dioritic and tonalitic rocks, a lower-grade garnet–clinopyroxene–plagioclase (Gt–Cpx–Pl) zone and patchy, higher-grade orthopyroxene zones are distinguished. Grade decreases abruptly to greenschist in the Abitibi subprovince to the east across the Ivanhoe Lake cataclastic zone. Grade decreases gradually through amphibolite to greenschist facies in the Wawa subprovince to the west. Based on mineral-melt equilibria, minimum conditions for the Gt–Cpx–Pl zone are 750°C, 6 kbar, a_{H_2O} = 0.5–0.7 and for the orthopyroxene zone, 770°C, 6 kbar, $a_{H_2O} < 0.5$.

Various garnet–biotite and garnet–pyroxene geothermometers and geobarometers yield apparent temperatures ranging from <600°C in the west to locally >800°C. Apparent pressure values derived from the pyrope–grossular–anorthite–diopside–quartz equilibrium are 5.4–8.4 kbar (average 6.3) and define a NNE-trending area of relatively high *P* in the eastern and central Kapuskasing Zone, supporting the interpretation of a tilted crustal section.

Introduction

Regional metamorphism variably affected rocks of the Superior Province over an area of ~3 × 10^6 km^2. The erosion level throughout the southern part of the province exposes metamorphic rocks of the greenschist and amphibolite facies except in the Kapuskasing Structural Zone, where pyroxene-bearing gneisses are associated with a linear gravity high (Innes, 1960; Bennett *et al.*, 1967; MacLaren *et al.*, 1968; Thurston *et al.*, 1977). The Kapuskasing Zone in the relatively well-exposed Chapleau-Foleyet area consists of a variety of migmatitic pyroxene–garnet–hornblende–biotite-bearing rocks. The assemblages preserved at the time of metamorphic quenching provide insight into reactions leading to the decomposition of hornblende and biotite in an amphibolite-granulite facies transition zone. The metamorphic history and equilibration conditions of rocks in the Kapuskasing Zone and adjacent Wawa subprovince are examined in this study.

Metamorphism in the Kapuskasing Zone is Archean as inferred from U-Pb dates on zircon from leucosome in paragneiss (2627±5 Ma) and on metamorphic zircon in mafic gneiss (2650±2 Ma) (Percival and Krogh, 1983).

Geological setting

The Superior Province can be divided into metavolcanic-plutonic and metasedimentary subprovinces (Stockwell, 1970) (Fig. 1). In the south-central Superior Province, the easterly trends of the Abitibi-Wawa and Quetico-Opatica subprovinces are transected over a distance of 500 km by the north–northeast-trending Kapuskasing Structural Zone (Thurston *et al.*, 1977) (Fig. 1). It is made up of gneisses in the upper amphibolite to granulite facies (Bennett *et al.*, 1967; MacLaren *et al.*, 1968) and is characterized by positive gravity and aeromagnetic anomalies over most of its length (Innes, 1960).

The Chapleau-Foleyet area straddles the Kapuskasing Zone and includes parts of the adjacent Abitibi and Wawa subprovinces. Supracrustal rocks of the Abitibi subprovince in the study area comprise mostly mafic metavolcanic flows and tuffs up to 6100 m thick (Goodwin, 1965). Easterly-trending belts of felsic metavolcanic and metasedimentary rock make up about 5 and 3% respectively of the supracrustal succession. Massive to foliated plutons of tonalite to granite composition (Streckeisen, 1976) range in diameter from ~1 to ~25 km. The intensity of metamorphism increases from the cores of supracrustal belts, where greenschist-facies assemblages are common (Thurston *et al.*, 1977), to contact areas with large intrusive bodies, where hornblende–plagioclase±garnet assemblages prevail. Both primary structures, including bedding and volcanic features, and sub-vertical tectonic foliation, schistosity and lineation, are present in the supracrustal succession.

The contact between rocks of the Abitibi subprovince and the Kapuskasing Structural Zone to the west is the Ivanhoe Lake cataclastic zone (Fig. 2), comprising blas-

0003–004X/83/0708–0667$02.00

Fig. 1. Lithotectonic subdivisions of the southern Canadian Sheild including subprovinces of the Superior Province (after Goodwin, 1977). Metasedimentary subprovinces are stippled.

tomylonite, cataclasite and pseudotachylite veinlets (Percival and Coe, 1981). These fault rocks are sporadically developed in rocks of the eastern 2 km of the Kapuskasing Zone and have random orientation within individual outcrops. The overall NNE trend is deduced from the distribution of fault rocks in the field.

The Kapuskasing Zone consists of ENE-striking belts of paragneiss, mafic gneiss, tonalitic and dioritic rocks and units of the Shawmere anorthosite complex (Thurston *et al.*, 1977; Percival, 1981a,b; Riccio, 1981). Paragneiss is layered, migmatitic, fine- to medium-grained, biotite–plagioclase–quartz rock, with some garnet and/or hornblende and/or orthopyroxene (Table 1). Concentrations of quartz, biotite, garnet, or graphite in some layers and the overall quartz-rich composition suggest that these rocks had a sedimentary origin. Mafic gneiss is a layered to homogeneous medium- to coarse-grained rock of high calcium (10.0–15.4 wt.% CaO), high-alumina (13.4–17.2 wt.% Al_2O_3) basaltic composition. It consists of Gt[1]–Cpx–Hb–Pl–Qz–Il±Opx±Sp±Sc assemblages and contains tonalitic leucosome veinlets on the 1–20 mm scale. Flaser diorite to mafic tonalite occurs as homogeneous to layered medium- to coarse-grained Hb–Bt–Pl±Qz±Cpx±Opx assemblages with up to 10% quartz and locally up to 15% concordant quartz monzonite veinlets. Rare gabbro and hornblendite layers may represent igneous differentiates. Tonalitic rocks are foliated to gneissic, locally xenolithic, consist of Bt–Pl–Qz±Hb±Gt assemblages, and contain paragneiss, mafic gneiss, and ultramafic (hornblendite or Gt–Opx–Hb rock) inclusions. Late hornblende–biotite tonalite dikes up to 50 cm thick transect gneissic layering in mafic and tonalitic gneiss. In 20-cm wide zones adjacent to these dikes, garnet, pyroxene-bearing assemblages are replaced by hornblende ±biotite assemblages. The Shawmere anorthosite complex (Fig. 2) comprises a main northern body, ~50 × 15 km, and a southern lens, ~15 × 4 km. The southern intrusion is homogeneous gabbroic anorthosite whereas the larger body contains anorthosite through gabbro units as well as some ultramafic rocks. The northern body is crudely zoned, consisting of a thin marginal unit of migmatitic amphibolite, a layered anorthosite–gabbro unit and a core of plagioclase-megacrystic gabbroic anorthosite (Riccio, 1981). A thin unit of foliated tonalite within the complex yielded a minimum U/Pb zircon date of 2765 Ma (Percival and Krogh, 1983) which provides a minimum age for the paragneiss-mafic gneiss country rock.

The western boundary of the Kapuskasing Zone is defined by the change in structural style and orientation from domal in the Wawa subprovince to northeasterly belts to the east (Fig. 2). Rare metaconglomerate in this boundary area has tonalitic cobbles with a U/Pb zircon date of 2664±6 Ma and a K–Ar hornblende date of 2594±151 Ma (Percival *et al.*, 1981).

The Wawa subprovince in the western part of the area (Fig. 2) is a tonalite to granodiorite gneiss terrane intruded by massive to foliated granite, quartz monzonite and tonalite plutons. The gneisses contain 0–25% amphibolitic enclaves as well as rare easterly-trending paragneiss units. Gneissosity is steep to subhorizontal, forming several domal structures, some with plutonic cores (Percival, 1981a). The Robson Lake dome, adjacent to the Kapuskasing Structural Zone (Fig. 2), has a core of mafic gneiss. Tonalite and granodiorite gneiss yield U/Pb zircon dates of >2707 and 2677 $^{+4.5}_{-2.8}$ Ma respectively (Percival and Krogh, 1983).

The age of metamorphism in the Abitibi and Wawa subprovinces is constrained by zircon dates on deformed, metamorphosed volcanics of 2749–2696 Ma (Turek *et al.*, 1982; Nunes and Pyke, 1980) and on post-metamorphic plutons of 2685–2668 Ma (Krogh and Turek, 1982; Krogh *et al.*, 1982). Concordant U–Pb zircon dates of 2650 and 2627 Ma from high-grade rocks of the Kapuskasing Zone indicate either a discrete younger metamorphic event or sustained metamorphic effects of the pre-2685 Ma event (Percival and Krogh, 1983).

Metamorphic zones

Mineral assemblages in each lithologic unit are listed in Table 1 and plotted in Figure 3. Assemblage data in the Abitibi subprovince in this area are not sufficient for delineation of isograds. Chlorite–white mica–albite–quartz assemblages characterize metasediments and epidote–chlorite–albite–quartz–carbonate±white mica± hornblende assemblages are common in mafic rocks (Thurston *et al.*, 1977). Hornblende–plagioclase±garnet assemblages occur in proximity to granitic plutons and locally near the Kapuskasing Zone.

Two high-grade metamorphic zones are recognized in the Kapuskasing Structural Zone and Wawa subprovince.

[1] Mineral abbreviations listed in Table 1.

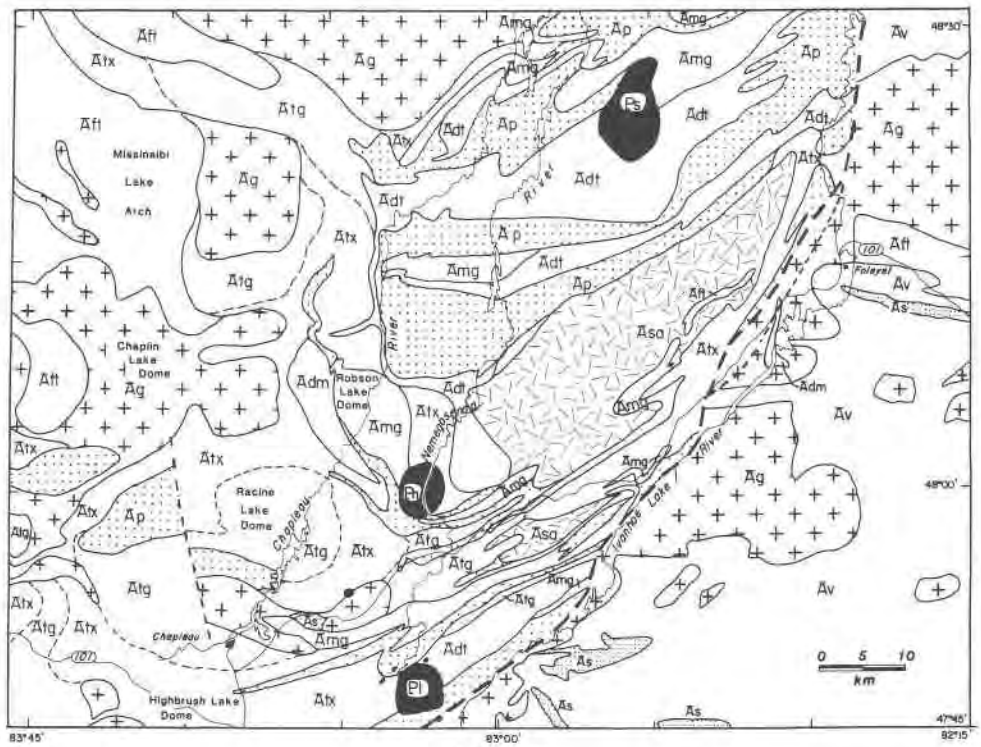

LEGEND

Proterozoic

- P — Alkalic rock–carbonatite complex: l: Lackner Lake complex; n: Nemegosenda Lake complex; s: Shenango complex — 1100 Ma intrusions

Archean

- A+g — massive granite, granodiorite, with minor tonalite
- Adm — diorite–monzonite intrusive complex; minor hornblendite, granite
- Aft — foliated to flaser tonalite
- Atg;x — tonalite–granodiorite gneiss; xenolithic — 2707–2668 Ma sequence
- Av — metavolcanic rocks, mainly metabasalt
- As — metasedimentary rocks (includes metaconglomerate with tonalite cobbles with a U-Pb zircon date of 2664±12 Ma) — 2749–2696 Ma sequence
- Adt — flaser diorite to mafic tonalite – includes minor gabbro, hornblendite, granodiorite — ?
- Asa — Shawmere anorthosite complex: metamorphosed gabbroic anorthosite, anorthosite, gabbro, minor tonalite
- Amg — mafic gneiss: high Ca,Al basaltic composition, with tonalitic leucosome — pre–2765 Ma sequence
- Ap — paragneiss– quartz-rich composition, with up to 15% tonalitic leucosome
- fault, Ivanhoe Lake cataclastic zone

Fig. 2. Generalized geological map of the Chapleau–Foleyet area (modified after Percival (1981b)). Geological boundary between the Kapuskasing Zone and Wawa subprovince is gradational in this area. Approximate boundary is Chapleau River south to Robson Lake dome, then Nemegosenda River south to Lackner Lake complex.

The Gt–Cpx–Pl zone, with diagnostic assemblages in mafic gneiss, extends from the Ivanhoe Lake cataclastic zone in the east, westward into the Wawa subprovince. In addition to the diagnostic minerals, mafic rocks contain brown hornblende, quartz, ilmenite and/or sphene, rare scapolite and ubiquitous tonalitic leucosome veinlets comprising variable proportions of quartz and plagioclase with minor hornblende, garnet or clinopyroxene. Para-

Table 1. Mineral assemblages and densities of rocks in Kapuskasing Structural Zone and eastern Wawa subprovince

Rock Type	S.G.	Ol	Sp	Gt	Sl	St	Sa	Opx	Cpx	Hb	Oa	M	Bt	Pl	K	Q	Sc	I	Sn	Cc	Cu
Mafic gneiss			±	x					x	x				x		x	x	x		±	
	3.10		±	x					x	x				x		x		x			
			±	x					x					x		x		x			
			±							x				x				x			
				x				x	x	x				x		x		x			
								x	x	x								x			
				x				x		x			x								
										x			x								x
Paragneiss						x						x	x	x		x					
	2.76			x									x	x		x					
(2.77)				x				x					x	x		x					
	2.83			x				x					x	x	x	x					
				x					x				x	x		x					
								x	x				x	x	x	x					
				x								x	x	x		x					
				x	x								x	x		x					
				x				x		x			x	x	x	x					
Dioritic gneiss (2.80)										x			x	x		x					
									x	x			x	x		x					
								x	x	x			x	x		x					
Anorthosite-suite rocks										x				x						±	
								x		x				x						±	
				x			x	x		x	x			x					x		
(2.82)		x						x	x	x									x		
		x		x				x		x				x							
								x	x	x				x							

Mineral abbreviations: Ol: olivine; Sp: sphene; Gt: garnet; Sl: sillimanite; St: staurolite; Sa: sapphirine; Opx: orthopyroxene; Cpx: clinopyroxene; Hb: hornblende; Oa: orthoamphibole; M: muscovite; Bt: biotite; Pl: plagioclase; K: K-feldspar; Q: quartz; Sc: scapolite; I: ilmenite; Sn: spinel; Cc: calcite; Cu: cummingtonite; S.G.: specific gravity (bracketed numbers refer to average values); ± designation indicates that small quantities of the mineral are present as an additional phase in some assemblages.

gneiss from this zone generally has Gt–Bt–Pl–Qz assemblages with tonalitic leucosome consisting of quartz and plagioclase (An_{27-35}) with minor biotite. Only one sillimanite occurence is known. Coarse muscovite is present in two localities near the margins of the Kapuskasing Zone, and one occurrence of staurolite–muscovite was noted (Fig. 3).

The orthopyroxene zone is represented by four areas with orthopyroxene-bearing rocks, surrounded by the Gt–Cpx–Pl zone. Isolated orthopyroxene localities and occurrences in anorthositic rocks, which may be igneous in origin, do not constitute orthopyroxene zones on Figure 3. In the orthopyroxene zone, small quantities of hypersthene occur, dominantly in paragneiss, but also in mafic and dioritic rocks. This implies that orthopyroxene forms in all rock types at similar grade, in contrast to the Adirondacks, where orthopyroxene forms in mafic rocks at lower grade than in felsic compositions (Buddington, 1963). In paragneiss, orthopyroxene, garnet and minor bleb antiperthite are locally present in leucosomes and orthopyroxene–K-feldspar–biotite occurs in melanosomes. Garnet, clinopyroxene and hornblende in specimen MG-20 are overgrown by fine symplectite of orthopyroxene–plagioclase, similar to the texture depicted by Horrocks (1980). This specimen contains three discrete plagioclase compositions: intergrowths of An_{35} and An_{50} occur in the matrix and An_{88} is present in symplectite.

Characteristic assemblages in lower-grade mafic rocks of the Wawa subprovince and Kapuskasing Zone are Hb–Pl–Qz±Sp±Il and Hb–Cpx–Pl–Qz; the approximate distribution of each assemblage is indicated in Figure 3. Felsic gneiss is made up of assemblages of Bt–Pl–Qz±Hb±Ksp. One occurrence each of Gt–Opx–Bt and Opx–Cpx–Pl are known from paragneiss. Assemblages of Gt–Cpx–Hb–Pl–Qz are common in the Robson Lake dome.

The transition from the Cpx–Hb–Pl zone, characteristic of the eastern Wawa subprovince, to the Gt–Cpx–Pl zone is not sharp. Where mafic gneiss with Gt–Cpx–Hb–Pl assemblages occurs as enclaves in gneiss, the xenolith margins have hornblende–plagioclase assemblages. Therefore, what may have been a prograde sequence has apparently been subsequently retrograded by felsic intrusions or retrogressing solutions.

With the exception of some orthopyroxene-bearing rocks with chlorite veinlets and cataclastic rocks altered to chlorite–epidote, the minerals in most specimens are fresh and are therefore suitable for chemical study.

Mineral chemistry

All mineral analyses were carried out on an ARL model AMX microprobe equipped with an energy dispersive detector set up and supervised by P. L. Roeder and M. I. Corlett at Queen's University. Operating conditions were

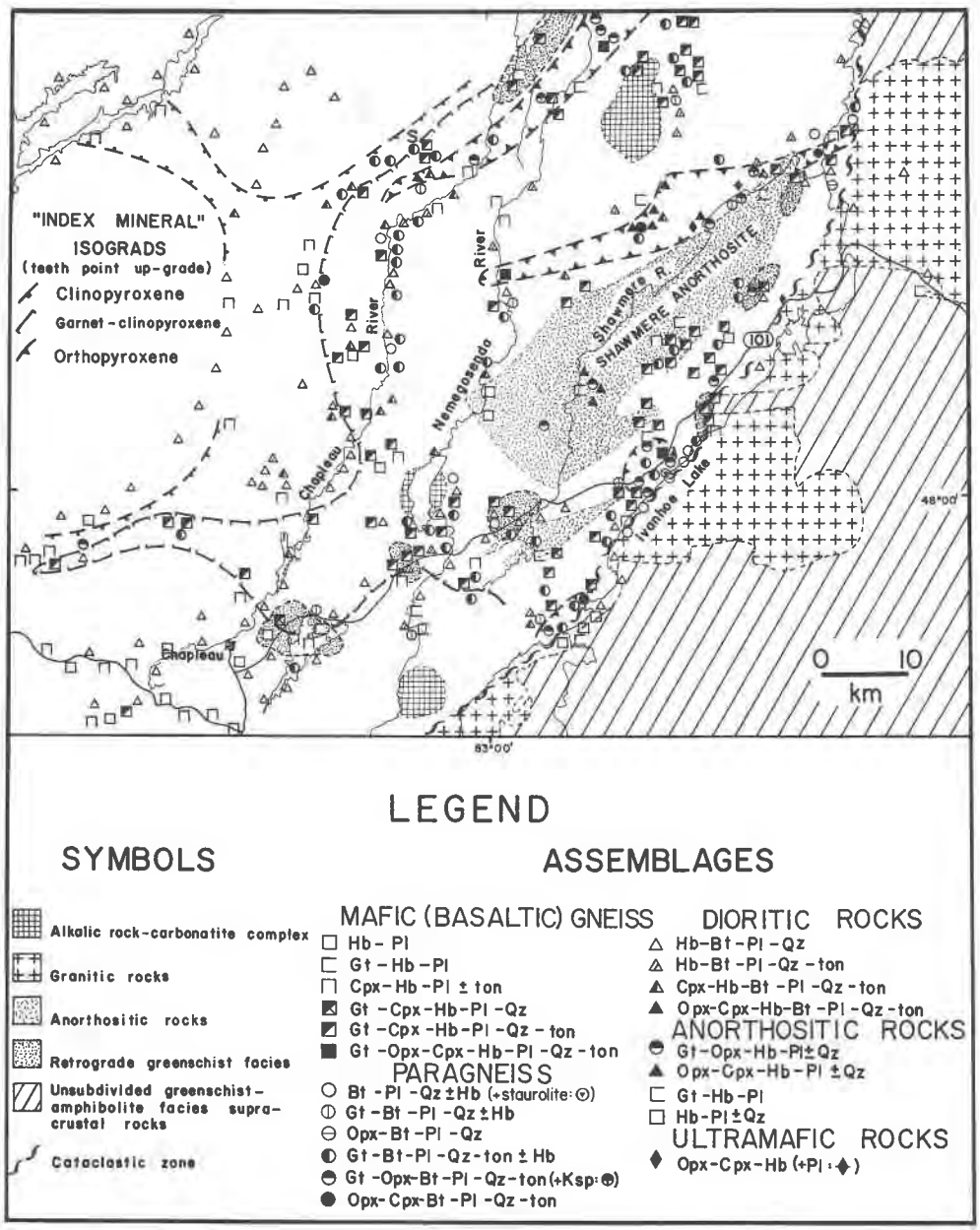

Fig. 3. Metamorphic mineral assemblages and index mineral isograds for part of the Chapleau–Foleyet area. Mineral abbreviations: Gt: garnet; Opx: orthopyroxene; Cpx: clinopyroxene; Hb: hornblende; Bt: biotite; Pl: plagioclase; Ksp:K-feldspar; Qz; quartz; ton: tonalitic segregations.

15 kV, 0.5 μA. Counting times of 120 seconds were used and data processed by an on-line minicomputer set up to apply Bence–Albee (1968) corrections and calculate weight per cent of oxides.

Between three and six spot analyses were made of each mineral in a probe section. Early detailed work showed that the average of three analyses is not significantly different from the average of six and therefore most of the results are averages of three analyses per mineral. Most minerals are homogeneous, with some chemical zonation within ~5 μm of the rim. Where rim composition is distinctly different from the interior analyses, it was excluded from the average.

Ten element analyses were recast into structural formulae according to the method of Deer *et al.* (1966). An estimate of Fe^{3+} content of garnet and pyroxene was made by assuming electroneutrality and adjusting Fe^{2+}/Fe^{3+} accordingly. Maximum and minimum Fe^{3+} contents of hornblende were calculated by a method analogous to that of Stout (1972) and then averaged.

Mineral compositions from 25 paragneiss specimens are given in Appendix 1[2] and some compositional parameters are listed in Table 2. Garnet in paragneiss varies in $Mg/(Mg+Fe^{2+})$ from 0.15 to 0.35. Grossular component constitutes 3–18 mol% and spessartine 1.1–11.7 mol%. Combined grossular–spessartine is generally 8–15 mol% with a few values as high as 25% (Table 2). Garnets are commonly zoned near the rim and the general pattern is toward increasing almandine (0–8 mol%) and spessartine (0–4 mol%) and decreasing pyrope (0–7 mol%) and grossular (0–3 mol%) components. The cores of grains are commonly homogeneous and the near-rim zonation may be a surface retrograde effect (*cf.* Lasaga *et al.*, 1977). Orthopyroxene in paragneiss has a range of $Mg/(Mg+Fe^{2+})$ of 0.44–0.62 and Al_2O_3 constitutes 0.9–3.5 wt.%. Biotite is characterized by $Mg/(Mg+Fe) = 0.35$–0.68 and contains up to 4 wt.% TiO_2. Plagioclase is in the range An_{24-35} with one exception of An_{66}. Analyses of coexisting garnet, orthopyroxene, biotite, K-feldspar and plagioclase from specimen PG-21 are presented in Table 3.

Mineral analyses from 34 mafic gneiss specimens are given in Appendix 1, and compositional parameters are listed in Table 4. Two of the specimens in the MG-series, MG-1 and MG-2, are skarns, but are included because of their grossular-rich garnet–clinopyroxene assemblages. Garnet in mafic gneiss is in the $Mg/(Mg+Fe^{2+}) = 0.13$–0.43 range and grossular component constitutes 18–34 mol%. Spessartine is less than 5 mol% and andradite component is less than 5 mol%, an exception being MG-2, with 20 mol% andradite. Garnets generally have homogeneous interiors but are weakly zoned immediately adjacent to the rim. Spessartine and grossular contents vary only slightly whereas almandine increases (0–5 mol%) and pyrope decreases (0–4 mol%) within 5–10 μm of the grain boundary. Clinopyroxene is salite, with $Mg/(Mg+Fe^{2+})$ values of 0.45–0.80. Jadeite and Ca-tschermakite components are in the 0–2.2 and 0–7.8 mol% ranges respectively. Amphiboles are common hornblende except for some secondary actinolite. Amphibole which appears to be part of the equilibrium assemblage is brown and richer in Al_2O_3 (10–12 wt.%) and TiO_2 (0.4–2.2 wt.%) than green amphibole of apparent retrograde origin (8–10 wt.% Al_2O_3; 0.03–0.56 wt.% TiO_2). An exception is secondary sodic amphibole from MG-30, with 4.15 wt.% TiO_2. Plagioclase is andesine to labradorite (An_{30}–An_{65}) and shows weak normal zoning. Two coexisting plagioclases in MG-20 (An_{35}, An_{50}) appear to be related by the Bøggild miscibility gap (Ribbe, 1975). Ilmenite contains less than 0.5 wt.% MgO. Scapolite has been noted in a few specimens, in one to the exclusion of plagioclase. Orthopyroxene is present in only two mafic gneiss specimens (MG-20, 22), and contains up to 4.7 wt.% Al_2O_3. Analyses of coexisting garnet, clinopyroxene, orthopyroxene and hornblende in specimen MG-20 are presented in Table 5.

Mineral analyses of dioritic, ultramafic and anorthosite-suite rocks are included in Appendix 1 and parameters listed in Table 6. Analyses of coexisting orthopyroxene, clinopyroxene, hornblende, biotite and plagioclase from a dioritic rock (OG-6) are presented in Table 7.

Graphical representation of assemblages

Minerals in mafic gneiss can be approximately represented in the system SiO_2–Al_2O_3–FeO–MgO–CaO–Na_2O–H_2O, by ignoring the minor amounts of Fe_2O_3 calculated for the mafic phases. At fixed pressure, temperature and a_{H_2O} and in the presence of quartz and plagioclase of constant composition, phase relations can be shown in terms of three components:

$$A = Al_2O_3 - (CaO + Na_2O)$$

$$F = FeO$$

$$M = MgO$$

Mineral compositions can thus be plotted on a diagram using A/F+M and M/F+M coordinates (Stout, 1972).

Projections of coexisting hornblende, clinopyroxene, orthopyroxene and garnet define a crossing tie-line (Fig. 4). Consequently, the four minerals are stable along a line in a P–T diagram if $a_{H_2O} = f(P,T)$; at lower temperature, hornblende and garnet are stable and at higher temperature, orthopyroxene and clinopyroxene are stable (Fig. 4). If water activity varies independently of P,T, a decrease in a_{H_2O} at constant temperature would favor the orthopyroxene–clinopyroxene assemblage.

The assemblage garnet–clinopyroxene–hornblende is stable over a P–T range, represented by a shifting triangle on Figure 4. The garnet–clinopyroxene zone is reached when the bulk composition of the rock falls into the garnet-clinopyroxene-hornblende field. The orthopyroxene zone is reached when the path of metamorphism intersects the reaction

$$\text{garnet} + \text{hornblende} \rightleftharpoons \text{orthopyroxene} + \text{clinopyroxene} \quad (1)$$

The path of metamorphism extends only slightly beyond this reaction because the incompatibility of garnet–hornblende is never fully established.

Pressures and temperatures of migmatite formation

Tonalitic veinlets, consisting of plagioclase (An_{27-35}), quartz and minor biotite, orthopyroxene, garnet, clinopyroxene or hornblende, occur in mafic rocks and in paragneiss as concordant layers and discrete pods. Several modes of origin are possible: 1) crystallization from

[2] Analyses listed in appendices may be obtained from the writer or order Document AM-83-228 from the Business Office, Mineralogical Society of America, 2000 Florida Avenue, N.W., Washington, D. C. 20009. Please remit $1.00 in advance for the microfiche.

Table 2. Paragneiss mineral composition and equilibria data

No.	Assemblage[A]	Metamorphic[B] Zone	X_{Mg}^{Gt}[C]	X_{Ca}^{Gt}[D]	X_{Mn}^{Gt}[E]	X_{Mg}^{Bt}[F]	$K_{D_{FeMg}}^{Gt-Bt}$[G]	X_{An}^{Pl}[H]	$X_{Al_2O_3}^{Opx}$[I]	X_{Fe}^{Opx}[J]	T(°C)[K]	P(kbar)[L]	$a_{H_2O}^{M}$	Comments
PG 1	Gt Hb Bt Pl Q I	3	0.147	0.167	0.069	0.415	0.244	0.315			710	(7.0)		
PG 2	Gt Bt Pl K Q	3	0.150	0.158	0.088	0.352	0.334	0.314			860	(7.0)		Antiperthite present T^N = 360°C
PG 3	Gt Hb Bt Pl Q I	2	0.151	0.168	0.079	0.436	0.229	0.661			685	(7.0)		
PG 4	Gt Bt Pl Q	3	0.156	0.096	0.083	0.402	0.274	0.481			765	(7.0)		
PG 5	Gt Bt Pl Q I	2	0.156	0.030	0.097	0.507	0.180	0.239			590	(7.0)		Green biotite
PG 6	Gt Bt Pl Q I	3	0.163	0.123	0.117	0.527	0.175	0.341			580	(7.0)		
PG 7	Gt Hb Bt Pl Q I	3	0.178	0.148	0.105	0.541	0.184	0.310			600	(7.0)		
PG 8	Gt Bt Pl K Q	3	0.187	0.180	0.066	0.546	0.191	0.308			610	(7.0)		T^P = 505°C
PG 9	Gt Bt M Pl Q I	3	0.189	0.042	0.053	0.514	0.221	0.273			670	(7.0)		
PG 10	Opx Cpx Bt Pl K Q I	4				0.452		0.359	0.022	0.450	820[Q]	(7.0)	0.186	T^P = 415°C
PG 11	Gt Hb Bt Pl Q I	3	0.196	0.188	0.058	0.511	0.234	0.400			690	(7.0)		
PG 12	Gt Bt Pl Q	1	0.197	0.074	0.077	0.491	0.254	0.311			730	(7.0)		
PG 13	Gt Opx Bt Pl Q I	4	0.198	0.059	0.062	0.523	0.225	0.312	0.028	0.463	675	9.9	0.067	P^T = 4.2 kbar
PG 14	Gt Bt Pl Q I	1	0.212	0.065	0.043	0.571	0.202	0.298			630	(7.0)		
PG 15	Gt Hb Bt Pl Q I	3	0.213	0.153	0.050	0.517	0.253	0.355			725	(7.0)		
PG 16	Gt Opx Hb Bt Pl Q I	4	0.214	0.166	0.037	0.544	0.228	0.349	0.031	0.470	680	6.5	0.094	T^N = 385°C; P^T = 6.4 kbar
PG 17	Gt Bt Pl Q	3	0.251	0.092	0.032	0.208	0.344				645	(7.0)		
PG 18	Gt Cpx Bt Pl Q	3	0.252	0.177	0.025	0.607	0.218	0.364			660	(7.0)		T^S = 650°C
PG 19	Gt Bt Pl Q I	3	0.256	0.066	0.026	0.594	0.235	0.302			695	(7.0)		
PG 20	Gt Opx Bt Pl Q I	4	0.269	0.110	0.017	0.637	0.225	0.316	0.083	0.565	675	-	0.368	P^T = 11.3 kbar
PG 21	Gt Opx Bt Pl K Q	4	0.304	0.150	0.014	0.638	0.247	0.300	0.066	0.398	715	3.1	0.315	Opx altered; P^T = 8.5 kbar; T^P = 560°C
PG 22	Gt Opx Bt Pl Q I	4	0.331	0.077	0.016	0.677	0.236	0.293	0.039	0.382	695	9.9	0.017	P^T = 8.1 kbar
PG 23	Gt Bt Pl Q I	3	0.323	0.104	0.019	0.666	0.238	0.265			700	(7.0)		
PG 24	Gt Sl Pl Q Bt	3	0.346	0.040	0.011	0.634	0.306	0.282			825	(6.7[R])		
PG 25	Gt Bt Pl Q I	3	0.350	0.077	0.025	0.641	0.302	0.301			815	(7.0)		

A: Mineral abbreviations as in Table 1
B: Metamorphic zones: 1: Hb-Pl; 2: Cpx-Hb-Pl; 3: Gt-Cpx-Pl; 4: Opx
C: X_{Mg}^{Gt} = (Mg/Mg + Fe) garnet
D: X_{Ca}^{Gt} = (Ca/Ca + Fe + Mn + Mg) garnet
E: X_{Mn}^{Gt} = (Mn/Ca + Fe + Mn + Mg) garnet
F: X_{Mg}^{Bt} = (Mg/Mg + Fe) biotite
G: $K_{D_{FeMg}}^{Gt-Bt} = \frac{(Mg/Fe)^{Gt}}{(Mg/Fe)^{Bt}}$
H: X_{An}^{Pl} = (Ca/Ca + Na + K) plagioclase
I: $X_{Al_2O_3}^{Opx}$ = (Al/Al + Fe + Mg) orthopyroxene
J: X_{Fe}^{Opx} = (Fe/Fe + Mg) orthopyroxene
K: based on Fe-Mg exchange between garnet and biotite (Ferry and Spear, 1978)
L: based on solubility of Al_2O_3 in orthopyroxene (Wood, 1974). Bracketed values are assumed
M: based on equilibrium (14)
N: orthopyroxene-ilmenite calibration (Bishop, 1980)
P: plagioclase-alkali feldspar calibration (Stormer, 1975)
Q: orthopyroxene-clinopyroxene calibration (Powell, 1978)
R: garnet-sillimanite-plagioclase-quartz calibration (Ghent et al., 1979)
S: garnet-clinopyroxene calibration (Ellis and Green, 1979)
T: based on equilibrium (11) (Perkins and Newton, 1981)

injected melt; 2) metamorphic differentiation; or 3) crystallization from *in situ* anatectic melt. The injected melt hypothesis is improbable because the pods and veinlets are generally isolated. In addition, the mafic mineral content of the veinlets is the same as that in the host. Both characteristics suggest local derivation. Metamorphic segregation was invoked by Amit and Eyal (1976) to explain quartz–plagioclase leucosome in the Wadi Magrish migmatites. This process is probable at sub-solidus temperatures (~630°C; Amit and Eyal, 1976), but is a more tenuous hypothesis for the present suite of rocks where indicated temperatures are much higher (see Geothermometry). Above 690°C at 5 kbar, in the presence of an aqueous fluid, which would be required to

Table 3. Microprobe analyses of minerals in PG-21

	1	2	3	4	5
SiO_2	38.48	48.38	37.56	64.08	60.98
TiO_2	0.04	0.04	3.90	0.63	0.05
Al_2O_3	21.42	2.64	16.25	19.47	25.97
Cr_2O_3	0.01	0.00	0.04	0.0	0.06
FeO*	28.94	24.34	15.23	0.15	0.0
MnO	0.76	0.18	0.06	0.12	0.02
MgO	8.03	17.71	15.05	0.51	0.52
CaO	2.89	0.51	0.10	0.04	6.20
Na_2O	0.02	0.89	0.57	0.86	7.90
K_2O	0.05	0.16	9.12	14.91	0.17
Total	100.64	94.34	97.90	100.67	100.91
Si	2.952	1.918	2.728	11.728	10.649
Aliv	0.00	0.082	0.272	4.205	5.345
Alvi	1.936	0.041	1.119		
Ti	0.002	0.001	0.213	0.085	0.005
Cr	0.001	0.00	0.002	0.0	0.008
Fe^{3+}	0.049	0.115	0.00		
Fe^{2+}	1.807	0.692	0.925	0.023	0.0
Mn	0.049	0.006	0.004	0.017	0.003
Mg	0.918	1.046	1.629	0.138	0.133
Ca	0.237	0.022	0.008	0.008	1.160
Na	0.003	0.068	0.080	0.304	2.673
K	0.005	0.008	0.845	6.963	0.037
(O)	(12)	(6)	(11)	(32)	(32)

1: garnet; 2: orthopyroxene; 3: biotite; 4: K-feldspar; 5: plagioclase

* *Total iron as FeO; Fe^{3+} by stoichiometry*
Specimen also contains quartz and secondary chlorite

transport the quartz and plagioclase components into the metamorphic segregation, quartz–plagioclase–H_2O should form a melt phase (Yoder, 1967). The modal composition of tonalite veinlets in the Kapuskasing migmatites (An_{27-35} (50–65%), quartz (35–50%)) is consistent with melt compositions in the 700–800°C range (Yoder, 1967). Crystallization from *in situ* trondhjemitic melt was similarly invoked by Ashworth (1976) to explain the absence of K-feldspar in leucosome of biotite–quartz–plagioclase migmatites.

Experimental anatexis of biotite–quartz–plagioclase rocks produces a granite minimum-melt composition (Brown and Fyfe, 1970; Winkler, 1979). The source of $KAlSi_3O_8$ component must be biotite (with quartz), implying biotite instability at temperatures less than 700°C and the presence of other reaction products, such as amphibole or orthopyroxene. This is in disagreement with the refractory nature of biotite in biotite–quartz–plagioclase assemblages (Clemens and Wall, 1981).

In quartz-bearing mafic rocks, anatectic melts are tonalitic in the range 690–900°C at P_{H_2O} = 5 kbar (Holloway and Burnham, 1972; Helz, 1976). The composition and proportion of plagioclase in tonalite veinlets from Kapuskasing mafic gneiss is consistent with an origin by crystallization from melt and therefore, a melt phase is considered to have coexisted with the solid phases at peak metamorphic conditions. By using the equilibrium relationship a_{H_2O} in melt = a_{H_2O} in vapor and assuming ideal mixing in the vapor and partitioning of H_2O into the melt (Kilinc, 1979), one can calculate the shift of dehydration reaction curve (2) caused by equilibrium with undersaturated melt of quartz diorite composition (*cf.* Eggler, 1972):

$$\underset{\text{in hornblende}}{4Ca_2Mg_5Si_8O_{22}(OH)_2} + \underset{\text{in plagioclase}}{3CaAl_2Si_2O_8}$$

$$\rightleftharpoons \underset{\text{in garnet}}{3Mg_3Al_2Si_3O_{12}} + \underset{\text{in clinopyroxene}}{11\ CaMgSi_2O_6} + \underset{\text{quartz}}{7SiO_2} + 4H_2O \qquad (2)$$

At any P,T, one can obtain:

$$\Delta G^\circ = -RT \ln \frac{a_{Py}^{Gt} \cdot a_{Di}^{Cpx} \cdot f_{H_2O}}{a_{Trem}^{Hb} \cdot a_{An}^{Pl}} - \Delta V_s(P - 1) \qquad (3)$$

Values of ΔG° and ΔV_s were obtained from Helgeson *et al.* (1978) and Haselton and Westrum (1980). The activity of Mg-components in minerals from four rocks spanning the range of compositional variation (X_{Mg}^{Gt} = 0.09–0.33) have been estimated from microprobe analyses and ideal ionic solution models. For the purpose of this calculation, $a_{An} = X_{An}$. By calculating the position of the curve for various values of a_{H_2O}, one can estimate the P–T stability field of garnet–clinopyroxene–hornblende assemblages in the presence of tonalite melt (Fig. 5). The calculations were performed by an APL computer program written by D. M. Carmichael of Queen's University. Although there are large uncertainties in the position of the dehydration curve, resulting from uncertainties in ΔG° values, the calculated curve has a similar shape and position to experimentally-determined amphibole-breakdown curves for similar compositions, reported by Allen *et al.* (1975). The vapor-absent melting reaction within the divariant field is:

$$\text{hornblende} + \text{plagioclase} \rightleftharpoons \text{garnet} + \text{clinopyroxene} + \text{tonalite} \qquad (4)$$

Two intersections between dehydration and water-undersaturated melting curves occur for water activity values in the range 0.4–1.0; the minimum value occurs at about 3 kbar and water activity increases to 1.0 at 0.5 and at 15 kbar. As temperature increases beyond the curve, the proportion of products increases and water activity decreases. The overall negative slope of the vapor-absent hornblende melting curve is a function of the shapes of granitic solidii (concave toward high P,T) and amphibole dehydration curves (concave toward low P). These curves intersect at two P,T points where a_{H_2O} is 1 by definition. The vapor-absent melting curve joining these two points has a negative slope, which is in contrast to the experimental vapor-absent melting curves for hornblende in acid and intermediate compositions of Brown and Fyfe (1970), which show strong positive dP/dT slopes. The

Table 4. Mafic gneiss mineral composition and equilibria data

No.	Assemblage[A]	Metamorphic[B] Zone	Garnet[C]				Clinopyroxene			T(°C)[G]	P(kbar)[H]	a_{H_2O}[I]	Comments
			X_{Mg}	X_{Fe}	X_{Ca}	X_{Mn}	X^{D}_{Mg}	X^{E}_{CaTs}	$X^{Pl\,F}_{An}$				
MG-1	Sp Gt Cpx Pl Q Cc	3	.011	.209	.677	.103	.546	.028	.483	705			Skarn
MG-2	Gt Cpx Q	3	.019	.230	.681	.070	.449	.103		895			Skarn
MG-3	Sp Gt Cpx Hb Q Sc I	3	.078	.510	.327	.085	.676	.052		725			prehnite present
MG-4	Sp Gt Cpx Hb Bt Pl Q I	3	.100	.626	.237	.04	.599	.024	.430	650	6.1	0.103	Amphibole coronas; T^{J} = 630°C
MG-5	Sp Gt Cpx Cu Hb Pl Q Sc I	4	.092	.572	.304	.031	.571	.061	.519	755	6.5	.0689	T^{K} = 580°C
MG-6	Sp Gt Cpx Hb Pl Q I Sc Cc	3	.088	.524	.343	.046	.567	.061	.498	800	7.3	1.312	Fine symplectite - Opx?
MG-7	Gt Cpx Hb Bt Pl Q I Ma Cc	3	.105	.607	.255	.033	.568	.050	.373	755	6.7	0.147	T^{L} < 500°C
MG-8	Gt E Cpx Hb Pl Q I Cc	3	.123	.644	.211	.022	.700	.050		690		0.401	Cataclastic
MG-9	Gt Cpx Hb Pl Q I	4	.114	.587	.260	.039	.576	.032	.300	745	7.8	0.147	
MG-10	Sp Gt Cpx Hb Pl Q I	3	.112	.555	.288	.045	.604	.055	.592	765	6.6	0.525	
MG-11	Sp Gt E Cpx Hb Pl Q	3	.114	.549	.304	.033	.635	.031	.775	740	6.0	0.853	Actinolite present
											5.5		
MG-12	Gt E Cpx Hb Pl Q I	3	.118	.561	.276	.046	.622	.077	.583	765	6.5	0.458	T^{M} = 515°C
MG-13	Gt Cpx Hb Pl Q I	3	.124	.582	.254	.041	.603	.037	.406	735	6.4	0.232	
MG-14	Sp Gt Cpx Hb Pl Q I Ma	3	.122	.557	.280	.039	.643	.075	.503	775	6.8	0.179	
MG-15	Sp Gt Cpx Hb Pl Q Sc I Cc	3	.126	.570	.272	.031	.632	.044	.523	740	6.2	0.361	
MG-16	Gt Cpx Hb Bt Pl Q I	3	.131	.581	.260	.029	.680	.099	.398	765	6.3	.0564	
MG-17	Gt Cpx Hb Pl Q I	3	.137	.606	.227	.030	.607	.037	.371	725	6.5	0.014	
MG-18	Sp Gt Cpx Hb Pl Q I	3	.136	.593	.248	.023	.645	.065	.334	750	7.3	0.256	
MG-19	Gt Cpx Hb Pl Q I	3	.149	.602	.225	.024	.636	.052	.330	725	7.0	0.235	T^{M} = 685°C
MG-20	Gt Opx Cpx Hb Pl Q I	4	.157	.601	.228	.013	.692	.078	.450	735	6.2	0.207	Opx-Pl coronas
												0.714	P^{N} < 0; P^{Q} = 9.1 kbar
MG-21	Gt Cpx Hb Pl Q I	3	.151	.566	.256	.027	.658	.056	.532	755	6.7	0.645	
MG-22	Gt Opx Cpx Hb Pl I	4	.164	.598	.182	.056	.668	.005	.360	655	3.9	0.294	P^{N} = 7.9 kbar; T^{R} = 785°C; P^{Q} = 6.0 kbar
MG-23	Sp Gt Cpx Hb Bt Pl Q I Cc	3	.194	.604	.205	.023	.692	.030	.404	685	5.4	0.070	T^{J} = 700°C
MG-24	Sp Gt E Cpx Hb Pl Q I	3	.159	.564	.244	.034	.686	.074	.482	755	6.9	0.604	
MG-25	Sp Gt Cpx Hb Bt Pl Q I	3	.149	.525	.300	.027	.680	.057	.650	755	7.2	0.722	
MG-26	Gt E Cpx Hb Bt Pl Q I	3	.172	.588	.205	.035	.664	.030	.375	725	6.1	0.114	Cataclastic
MG-27	Gt Cpx Hb Pl Q I	4	.176	.598	.198	.028	.668	.056	.372	725	6.2	0.235	T^{M} = 610°C
MG-28	Gt Cpx Hb Pl Q I	3	.195	.606	.192	.016	.718	.073	.421	715	5.9	0.426	
MG-29	Gt Cpx Hb Pl Q I Cc	4	.204	.538	.218	.039	.757	.054	.460	715	6.5	0.305	
MG-30	Gt Cpx Hb Bt Pl Ma Cc	3	.199	.506	.256	.039	.797	.054		760		0.475	Riebeckite present; T^{J} = 760°C
MG-31	Gt Cpx Hb Bt Pl Q I	3	.225	.565	.193	.017	.725	.051	.480	720	6.0	0.182	
MG-32	Gt Cpx Hb Pl Q I	3	.334	.436	.208	.023	.802	.049	.523	810	8.3	0.506	

A: Mineral abbreviations as in Table 1; also Ma: magnetite; E: epidote
B: Metamorphic zones: 3: Gt-Cpx-Pl; 4: Opx
C: Mole fraction (X) of component i = i/i + j + k + l
D: X_{Mg} = Mg/Mg + Fe in clinopyroxene
E: X_{CaTs} = Al IV - [Ti] ÷ Σ Clinopyroxene end-members
F: X^{Pl}_{An} = Ca/Ca + Na + K in plagioclase
G: based on Fe-Mg partitioning between garnet and clinopyroxene (Ellis and Green, 1979)
H: based on equilibrium (10) (Perkins and Newton, 1981)
I: based on equilibrium (2)
J: based on Fe-Mg partitioning between garnet and biotite (Ferry and Spear, 1978)
K: scapolite-plagioclase calibration (Goldsmith and Newton, 1976)
L: ilmenite-magnetite calibration (Buddington and Lindsley, 1964)
M: ilmenite-clinopyroxene calibration (Bishop, 1980)
N: garnet-orthopyroxene calibration (Wood, 1974)
Q: based on equilibrium (11) (Perkins and Newton, 1981)
R: two pyroxene calibration (Powell, 1978)

Table 5. Microprobe analyses of minerals in MG-20.

	1	2	3	4
SiO_2	38.01	51.57	49.06	42.29
TiO_2	0.00	0.34	0.03	2.03
Al_2O_3	20.99	2.92	4.75	12.98
Cr_2O_3	0.22	0.21	0.34	0.08
FeO*	28.06	11.81	31.20	18.43
MnO	0.70	0.00	0.81	0.17
MgO	4.11	11.34	13.35	9.28
CaO	8.32	22.65	1.39	11.41
Na_2O	0.27	0.74	0.52	1.95
K_2O	0.00	0.08	0.00	0.69
Total	100.67	101.79	101.45	99.31
Si	2.973	1.908	1.885	6.252
Aliv	0.00	0.092	0.115	1.748
Alvi	1.935	0.035	0.100	0.513
Ti	0.00	0.009	0.001	0.226
Cr	0.014	0.008	0.010	0.009
Fe^{3+}	0.0	0.087	0.042	0.288
Fe^{2+}	1.835	0.278	0.960	1.990
Mn	0.040	0.003	0.026	0.021
Mg	0.479	0.625	0.764	2.044
Ca	0.697	0.898	0.057	1.807
Na	0.041	0.053	0.039	0.559
K	0.00	0.004	0.00	0.130
(O)	(12)	(6)	(6)	(23)

1: garnet; 2: clinopyroxene; 3: orthopyroxene; 4: hornblende

* *Total iron as FeO; Fe^{3+} by stoichiometry*
Specimen also contains quartz and plagioclase ($An_{33,57}$ in matrix, An_{88} in symplectite)

reason for the discrepancy between experiments and calculations may be that tremolite with ideal ionic substitutions is an inadequate model for high-grade hornblende.

The stability contours for Reaction 4 intersect Reaction 5 and generate equivalent stability contours for the assemblage orthopyroxene–clinopyroxene–garnet in the orthopyroxene zone (Fig. 5):

orthopyroxene + anorthite $\rightleftharpoons$ garnet

$$+ \text{ clinopyroxene} + \text{quartz} \qquad (5)$$

The P–T position of $X_{Mg}^{Gt} = 0.09$–0.33 stability contours for Reaction 5 were estimated by first calculating the Fe:Mg ratio of orthopyroxene which would be in equilibrium with garnet using an average Gt–Opx Fe–Mg distribution coefficient of 3.46 then calculating the P–T conditions defined by the assemblage according to Hansen (1981). This provides a minimum pressure at specified temperature in the absence of orthopyroxene. The intersection of stability contours for Reactions 4 and 5 defines the position of Reaction 1.

Paragneiss in the Gt–Cpx–Pl zone generally contains Gt–Bt–Pl–Qz assemblages and tonalitic leucosome. The first appearance of orthopyroxene can be related to a biotite-consuming reaction:

biotite + quartz $\rightleftharpoons$ orthopyroxene

$$+ \text{ K-feldspar} + H_2O \qquad (6)$$

The downward shift in the position of the dehydration curve as a result of coexistence with water-undersaturated melt has been calculated for (6) with natural mineral compositions in the same manner as for (2). The locus of intersection of equal a_{H_2O} for (6) and the tonalite solidus yields a vapor-absent melting curve along which the generalized reaction is:

biotite + quartz + plagioclase

$$\rightleftharpoons \text{orthopyroxene} + \text{granodiorite} \qquad (7)$$

The initial melt composition in the leucosomes is tonalitic but becomes granodioritic after K-feldspar is produced by decomposition of biotite, in accord with the observation of up to 10% antiperthite in leucosome of orthopyroxene-bearing paragneiss.

The curve (Fig. 6) has a steep positive dP/dT slope and assuming P of 6 kbar, orthopyroxene is stable above 770°C, in agreement with the experiments of Wendlandt (1981) and Clemens and Wall (1981).

The preceding discussion has assumed a closed system and equilibrium between melt and solids, however it is difficult to explain the presence of fresh orthopyroxene in tonalite veinlets if the system remained closed until crystallization. Reactions between water dissolved in the melt and orthopyroxene should yield hydrous phases. Hence water is considered to have been removed or diluted during or prior to crystallization. Removal could have been accomplished by collection and upward migration of tonalitic liquids leaving a water-depleted residue. The origin of many Archean tonalites has been ascribed to partial melting of mafic rocks containing garnet–clinopyroxene–quartz (Arth and Hansen, 1972) or garnet-clinopyroxene-orthopyroxene-plagioclase (Gower *et al.*, 1982). Alternatively, dilution of the ambient fluid by externally-derived CO_2-rich vapors (Weaver, 1980; Friend, 1981; Janardhan *et al.*, 1982) could induce crystallization and prevent retrogression, in the manner outlined by Wendlandt (1981).

Superimposed on Figure 6 is the vapor-phase absent melting curve for mafic rocks. The two curves intersect near 6 kbar, 775°C for natural compositions. This implies that in regional metamorphic terranes characterized by pressure above this intersection, hornblende will start to react to form garnet–clinopyroxene-melt at temperatures where paragneiss may be migmatitic but contains no orhtopyroxene. In lower-pressure environments, biotite will become unstable at lower grade than hornblende, or hornblende may be involved in reactions producing orthopyroxene in mafic rocks (*cf.* Wells, 1979).

Minimum pressure–temperature conditions were de-

Table 6. Orthogneiss mineral composition and equilibria data

No.	Assemblage[A]	Metamorphic Zone[B]	X_{Mg}^{Gt}[C]	X_{Ca}^{Gt}[D]	X_{Mg}^{Opx}[E]	X_{Al}^{Opx}[F]	X_{Mg}^{Cpx}[G]	X_{An}^{Pl}[G]	T(°C)[I]	P(kbar)[J]	a_{H_2O}	Comments
OG-1	Gt Sa Opx Hb Oa Pl Sn	3	0.561	0.09	0.81	0.098		0.94	(750)	5.3		Anorthosite-suite Melagabbro
OG-2	Opx Cpx Hb Bt Pl	2			0.80	0.038	0.92		580	(7.0)	0.01	Ultramafic
OG-3	Gt Opx Hb Pl	3	0.592	0.12	0.82	0.072		0.94	(750)	7.0		Anorthosite-suite Melagabbro
OG-4	Gt Opx Hb	4	0.382	0.16	0.66	0.055			(750)	6.2		Ultramafic xenolith
OG-5	Opx Cpx Hb Bt Pl I Cc	4			0.741	0.044	0.84	0.44	750	(7.0)	0.11	Ultramafic
OG-6	Opx Cpx Hb Bt Pl Q	4			0.62	0.022	0.77	0.36	730	(7.0)	0.06	Diorite
OG-7	Ol Opx Cpx Hb Sn	4			0.88	0.017	0.870		610	(7.0)	0.05	Mg-rich Ultramafic; T^L = 800°C
OG-8	Opx Cpx Hb Pl	3			0.71	0.035	0.820	0.88	740	(7.0)		Anorthosite-suite gabbro

A: *Mineral abbreviations as in Table 1*
B: *Metamorphic zones: 2: Cpx-Hb-Pl; 3: Gt-Cpx-Pl; 4: Opx*
C: $X_{Mg}^{Gt} = (Mg/Mg + Fe^2)$ *garnet*
D: $X_{Ca}^{Gt} = (Ca/Ca + Mn + Mg + Fe^2)$ *garnet*
E: $X_{Mg}^{Opx} = (Mg/Mg + Fe^2)$ *orthopyroxene*
F: $X_{Al}^{Opx} = (Al/Al + Ca + Fe^2 + Mg)$ *orthopyroxene*
G: $X_{Mg}^{Cpx} = (Mg/Mg + Fe^2)$ *clinopyroxene*
H: $X_{An}^{Pl} = (Ca/Ca + Na + K)$ *plagioclase*
I: *based on Powell's (1978) two-pyroxene thermometer. Bracketed values are assumed for the pressure calibration*
J: *based on Wood's (1974) aluminous orthopyroxene-garnet barometer. Bracketed values are assumed for the temperature calibration*
K: *based on equilibrium (13)*
L: *based on Roeder et al. (1979) olivine-spinel thermometer*

fined in the previous section by solid–melt equilibria for the Gt–Cpx–Pl zone and for the orthopyroxene zone. Regional variation in apparent *P–T* conditions is now examined, based on calibrated geothermometers and geobarometers applied to individual samples. (Tables 2, 4 and 6)

Temperature estimation methods

Geothermometers based on Fe–Mg exchange between mineral pairs are sensitive to temperature variation and only slightly pressure-dependent. Therefore, to evaluate temperature-variation on a first approximation basis, a value of 7 kbar was initially estimated for all specimens. This value cannot be so precisely estimated but is shown below to be a reasonable average for the area.

The mineral pairs most suitable for geothermometry by virtue of widespread distribution and unaltered character are garnet–biotite and garnet–clinopyroxene. The Ferry and Spear (1978) experimental calibration of the garnet–biotite thermometer has gained general acceptance (*e.g.*, Ghent *et al.*, 1979; Ferry, 1980). Similarly, of the recently published garnet–clinopyroxene geothermometers (Raheim and Green, 1974; Ellis and Green, 1979; Saxena, 1979; Ganguly, 1979), the experimental calibration of Ellis and Green (1979), which takes account of the effect of calcium on Fe–Mg distribution, is well-suited for the study of the Kapuskasing Zone mafic rocks whose garnets contain up to 34 mol% grossularite. Mineral compositions meet the compositional restrictions imposed in both garnet–biotite and garnet–clinopyroxene calibrations (Appendix 1).

Figure 7 shows temperature estimates of the Ferry and Spear calibration plotted against estimates by the three most recent garnet–clinopyroxene calibrations for four rocks from the Kapuskasing Zone that contain all three minerals. Internal consistency is best for these samples for the Ellis and Green and Ferry and Spear calibrations. Both are experimentally-derived equations and take account of pressure effects. The agreement between the two techniques is in contrast to that reported for Adirondack granulites studied by Bohlen and Essene (1980).

Stoichiometric estimation of Fe^{3+} in biotite from probe data is not possible because site vacancies in biotite leave the structural formula cation-deficient. However, wet chemical analyses of biotite consistently indicate the presence of Fe_2O_3. To assess the partitioning of Fe^{3+}

Table 7. Microprobe analyses of minerals in OG-6

	1	2	3	4	5
SiO_2	52.28	51.83	43.49	36.83	58.45
TiO_2	0.15	0.24	2.02	6.07	0.03
Al_2O_3	0.98	1.99	10.92	14.07	24.79
Cr_2O_3	0.04	0.16	0.08	0.12	0.10
FeO*	24.53	8.79	14.1	15.16	0.13
MnO	0.86	0.16	0.23	0.03	0.04
MgO	21.24	13.53	12.09	13.54	0.00
CaO	0.38	21.20	11.25	0.03	7.05
Na_2O	0.38	0.73	1.57	0.00	6.75
K_2O	0.00	0.08	1.51	9.79	0.26
Total	100.51	98.74	97.28	95.65	97.62
Si	1.956	1.949	6.466	2.757	10.669
Aliv	0.004	0.007	1.534	0.243	5.333
Alvi	0.043	0.051	0.379	0.998	
Ti	0.00	0.038	0.226	0.341	0.004
Cr	0.001	0.005	0.009	0.006	0.013
Fe^{3+}	0.038	0.052	0.226	0.00	0.0
Fe^{2+}	0.729	0.225	1.527	0.949	0.019
Mn	0.027	0.005	0.029	0.001	0.005
Mg	1.184	0.758	2.679	1.510	0.00
Ca	0.015	0.854	1.791	0.002	1.379
Na	0.002	0.053	0.452	0.00	2.388
K	0.00	0.004	0.286	0.935	0.06
(O)	(6)	(6)	(23)	(11)	(32)

1: orthopyroxene; 2: clinopyroxene; 3: hornblende; 4: biotite; 5: plagioclase
* *Total iron as FeO*
Specimen also contains quartz

between coexisting garnet and biotite, wet chemical analyses from several sources were used. Reinhardt's (1968) analyses indicate that on the average the $Fe^{3+}/(Fe^{2+} + Fe^{3+})$ ratio in biotite is 2.4% larger than that in coexisting garnet. Lal and Moorhouse (1969) present data which indicate that the $Fe^{3+}/(Fe^{2+} + Fe^{3+})$ ratio in biotite is 8.4% higher than that of coexisting garnet, and Chinner's (1960) data indicate a wide range, from 4 to 22%, with an average of 12.4% larger $(Fe^{3+}/(Fe^{2+} + Fe^{3+})$ in biotite than garnet. The effect on geothermometric measurement of assuming 8.4% more Fe^{3+}/Fe_{total} in biotite than in garnet as calculated stoichiometrically, is negligible (apparent change of −1°C using Ferry–Spear calibration). Assuming a 12% average, the difference is only −2°C.

The agreement between the garnet–clinopyroxene and garnet–biotite thermometers is best when all iron is assumed to be Fe^{2+} in garnet, biotite and clinopyroxene for both thermometers (Fig. 7) and the calculations in Tables 2, 4 and 6 are based on this procedure. Treating all iron as Fe^{2+} is actually an empirical correction used to achieve consistency between geothermometers (Fig. 7) and contrasts with the procedure of Raheim and Green (1975), who used calculated Fe^{2+} contents. The pyroxene commonly has larger Fe^{3+}/Fe_{total} than coexisting garnet and temperatures up to 100°C lower result if the calculated Fe^{2+} value is used to calculate K_D. Further justification for using total Fe rather than Fe^{2+} comes from samples MG-17 and MG-25, whose garnet and clinopyroxene contain no Fe^{3+} as calculated stoichiometrically. Temperatures of 725 and 755°C are in the same range as values calculated by ignoring Fe^{3+} in other specimens (Table 4).

A calibration of the two-pyroxene thermometer, proposed by Powell (1978), yields results which are consistent with garnet–biotite and garnet–clinopyroxene temperatures for the Kapuskasing gneisses. The equations formulated by Kretz (1982) give averaged values in the same range but some pyroxene pairs yield temperatures that are up to 100°C discordant. The Wood and Banno (1973) and Wells (1977) calibrations consistently give temperatures some 200–300°C higher.

Additional results were obtained for rocks containing mineral assemblages without widespread distribution (Tables 2, 4 and 6). In general, oxide, feldspar and ilmenite–pyroxene thermometers yield temperatures some 200–300°C lower than those estimated by the Fe–Mg exchange thermometers. No generalizations regarding other thermometers are possible because of the limited number of occurrences.

Regional temperature variation

Near-rim garnet analyses generally give results lower by 10–20°C than analyses of the relatively homogeneous interiors. The general analytical strategy was to check all

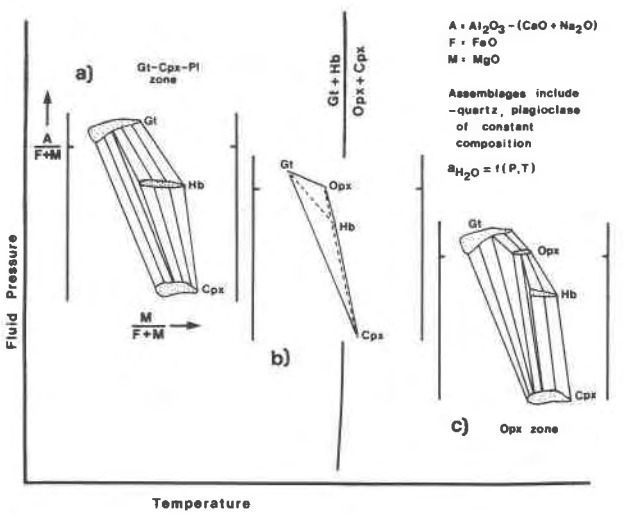

Fig. 4. Phase relations of mineral assemblages coexisting with tonalitic melt in mafic rocks. Mineral compositions are generalized from Appendix 1 for a and c; plotted from Table 5 for b. (a) garnet–clinopyroxene–hornblende compositional triangles shift to the right along M/M+F axis in response to rising temperature; (b) garnet + hornblende react to produce orthopyroxene + clinopyroxene with increasing temperature (or decreasing a_{H_2O} if P, a_{H_2O} are independent of T); (c) stable mineral assemblages in the orthopyroxene zone.

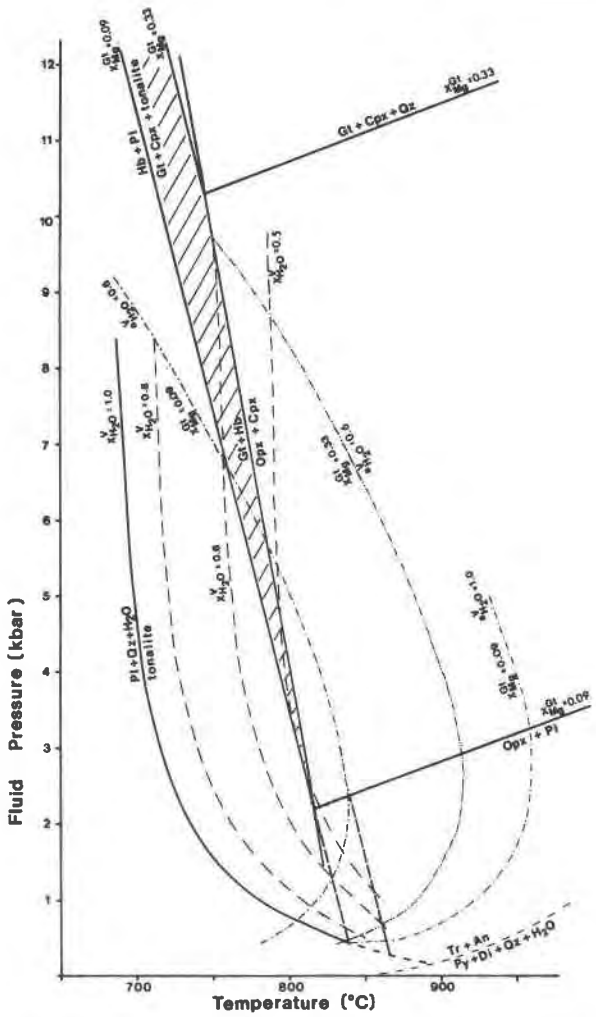

Fig. 5. Vapor-phase-absent-melting curve (diagonal ruling) corresponding to the reaction Hb + Pl = Gt + Cpx + tonalite for mafic rocks of variable Mg/(Mg+Fe) ratio. The curve is defined by the locus of intersection between dehydration (Reaction 2; dot–dash symbol) and melting (Kilinc, 1979) curves of equal water activity. Position of curves for reaction Opx + Pl = Gt + Cpx + Qz at variable X_{Mg}^{Gt} are based on Hansen (1981; p. 239) Symbols as for Fig. 3 except Py: pyrope; Tr: tremolite; Di: diopside; An: anorthite.

grains for zoning but exclude near-rim analyses from the average.

The results of the combined garnet–biotite, garnet–clinopyroxene and two-pyroxene thermometers are plotted in Figure 8, which shows an overall temperature range of 580–825°C. The extremes in this range are garnet–biotite temperatures; garnet–clinopyroxene results have a narrower spread (655–815°C). Much of the area without data points is underlain by diorite or tonalite orthogneiss without relevant assemblages.

The apparent temperature distribution of Figure 8 indicates two zones above 800°C in the northern part of the area as well as isolated occurrences in the 800°C range near the southeastern margin of the Kapuskasing Zone. Most of the Gt–Cpx–Pl zone is characterized by values above 700°C. Rocks which give apparent lower temperatures, in the 600°C range, are in the southwest corner of the area, where garnet-, biotite-bearing paragneiss schlieren occur as inclusions in tonalitic gneiss.

A high paleotemperature zone is present near the northern end of the Shenango complex (Fig. 2) and a possibly similar relationship exists east of the Nemegosenda Lake complex. The origin of the apparent thermal highs may relate to the late (1100 Ma) intrusive bodies. Samples from the vicinity of the Nemegosenda complex may have been affected by contact metamorphism, metasomatism, or crustal buckling or displacement adjacent to the body. Any of these processes could alter the apparent temperature of adjacent rocks, the first by readjusting Fe–Mg ratios of garnet and clinopyroxene, the second by increasing Ca content of garnet, and the third by displac-

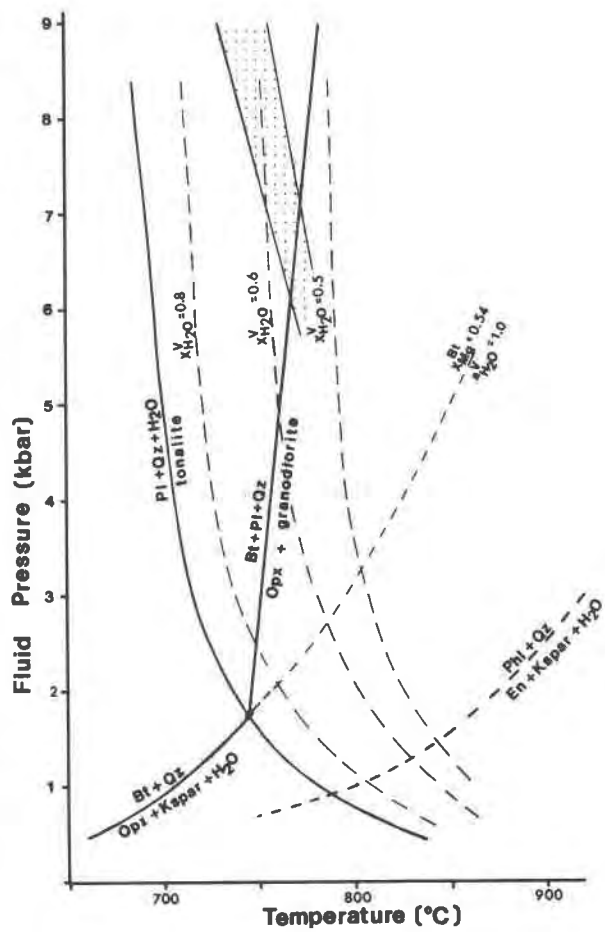

Fig. 6. Vapor-phase–absent-melting curve for paragneiss. Construction as for Fig. 5. Stippled area is VPAM curve for mafic rocks. Note that the two VPAM curves intersect at 6–8 kbar, 775°C for natural compositions.

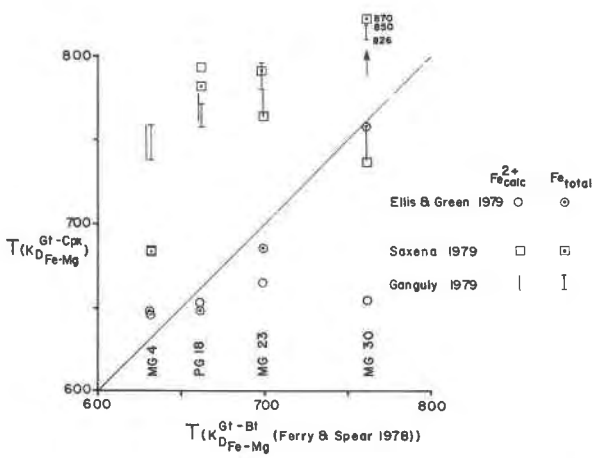

Fig. 7. Comparison of temperature estimates derived from garnet-biotite and various garnet–clinopyroxene thermometers. The two thermometers are consistent if the Ferry and Spear (1978) and Ellis and Green (1979) calibrations are used and K_D is calculated using the total iron content rather than stoichiometrically-determined Fe^{2+}.

ing deeper, presumably once-hotter rocks, to higher levels. Sample MG-2 from east of the Nemegosenda complex has local skarn mineral assemblages, including grossular, andradite-rich garnet and Fe-rich clinopyroxene, possibly suggesting metasomatic effects. A rock from south of the same body contains abundant biotite and riebeckite, possibly indicating introduction of alkalies during alkalic magmatic activity. Fenites are common adjacent to the Nemegosenda complex (Parsons, 1961). However, the width of the thermal aureole is difficult to estimate.

Excluding the temperature highs possibly associated with the younger intrusions, some of the patterns can be related to structural effects. For example, apparent temperatures of 705–755°C in the Robson Lake dome suggest possible late tectonic upwarping of isotherms around the dome. The role of doming in exposing supracrustal rocks west of the Kapuskasing zone has been discussed previously (Percival, 1981a).

A comparison between the *T*-estimates (Fig. 8) and the assemblage map (Fig. 2) shows little similarity between patterns. For example, the easterly-trending orthopyroxene zone in the center of the Kapuskasing Zone of Figure 3 is on strike with an apparent thermal low in the 600–700°C range. However, sample MG-22 yields discordant garnet–clinopyroxene and two-pyroxene temperatures of 655 and 785°C respectively. Orthopyroxene-bearing rocks to the north are not associated with thermal highs. In the southeastern Kapuskasing Zone, orthopyroxene-bearing rocks yield high apparent temperatures (>800°C) derived by the two-pyroxene (Powell, 1978) and garnet–biotite thermometers.

In the northern Kapuskasing Zone where assemblages are at variance with temperature data, it is likely that the Fe–Mg ratios in minerals used in the thermometers have equilibrated under different conditions than those at which the assemblages were stable. Alternatively, low water fugacity may have stabilized orthopyroxene at relatively low temperatures. However, at temperatures as low as 650°C and with low water fugacity, the production of partial melts would not be possible (Robertson and Wyllie, 1971). Because migmatite veinlets are ubiquitous in paragneiss in this region, a low-temperature origin is unlikely and retrograde Fe–Mg exchange seems to be a better explanation. Alternatively, biotite may have been in solution in the liquid phase while rocks were at temperatures above the solidus and crystallized upon later cooling to ~650°C. However, there is no textural evidence that this process occurred.

Metagabbros of the Shawmere complex locally consist of the assemblage Opx–Cpx–Hb–Pl (*e.g.*, OG-8, Table 6). Orthopyroxene occurs as homogeneous grains whereas clinopyroxene has two habits; large (up to 5 mm) grains have fine exsolution lamellae, and smaller matrix grains are optically and chemically homogeneous. Lamellae in the large grains are bent and offset, giving the complex grains undulose extinction. Chemically, the host clinopyroxene crystal ($Ca_{0.47}Fe_{0.10}Mg_{0.43}$) is identical in composition to the matrix clinopyroxene. The exsolved lamellae have the composition $Ca_{0.18}Fe_{0.21}Mg_{0.61}SiO_3$. By using a defocussed microprobe beam technique, analyses of the bulk composition of the clinopyroxene megacrysts were obtained. The bulk composition ($Ca_{0.40}Fe_{0.11}Mg_{0.49}$) is slightly poorer in calcium than matrix clinopyroxene. Bohlen and Essene (1978) interpreted pyroxenes with

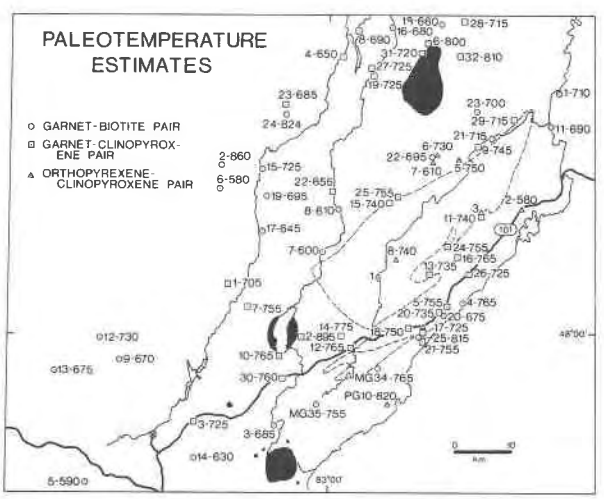

Fig. 8. Paleotemperature map of part of the Chapleau–Foleyet area. Temperatures estimated by garnet–biotite (Ferry and Spear, 1978), garnet–clinopyroxene (Ellis and Green, 1979) and two-pyroxene (Powell, 1978) thermometry. Numbers to the left of dash are sample identifiers; numbers to the right are in °C. circles: PG-series; squares: MG-series; triangles: OG-series.

exsolution lamellae in metamorphosed Adirondack anorthosite massifs as being of igneous derivation. They derived temperatures both of igneous crystallization (~1100±100°C) and metamorphism (~750°C) by reintegration of pyroxene compositions. The same treatment cannot be applied to the Shawmere metagabbro because orthopyroxene is homogeneous and plots in the metamorphic temperature range on Ross and Huebner's (1975) pyroxene solvus isotherm diagram. Assuming, however, that the exsolved clinopyroxene megacrysts at one time coexisted with a calcium-richer orthopyroxene, a temperature on the order of 1050°C can be estimated for igneous crystallization. Based on the composition of matrix clinopyroxene and homogeneous orthopyroxene, an estimated temperature of metamorphism of 750°C may be obtained from the Ross and Huebner isotherm plot.

Pressure estimation methods

Pressure estimates are dependent on the temperatures derived in the previous section. Several pressure-sensitive equilibria are relevant to assemblages with widespread distribution in the Kapuskasing Zone. The compositions of minerals in garnet–pyroxene–plagioclase–quartz parageneses are determined by equilibria, including:

$$\underset{\text{in plagioclase}}{CaAl_2Si_2O_8} \rightleftharpoons \underset{\text{in clinopyroxene}}{CaAl_2SiO_6} + \underset{\text{quartz}}{SiO_2} \quad (8)$$

$$\underset{\text{in garnet}}{2Ca_3Al_2Si_3O_{12}} + \underset{\text{in garnet}}{Mg_3Al_2Si_3O_{12}} \rightleftharpoons \underset{\text{in clinopyroxene}}{3CaMgSi_2O_6} + \underset{\text{in clinopyroxene}}{3CaAl_2SiO_6} \quad (9)$$

$$\underset{\text{in plagioclase}}{CaAl_2Si_2O_8} + \underset{\text{in clinopyroxene}}{CaMgSi_2O_6} \rightleftharpoons \underset{\text{in garnet}}{2/3Ca_3Al_2Si_3O_{12}} + \underset{\text{in garnet}}{1/3Mg_3Al_2Si_3O_{12}} + \underset{\text{quartz}}{SiO_2} \quad (10)$$

$$\underset{\text{in plagioclase}}{CaAl_2Si_2O_8} + \underset{\text{in orthopyroxene}}{Mg_2Si_2O_6} \rightleftharpoons \underset{\text{in garnet}}{1/3Ca_3Al_2Si_3O_{12}} + \underset{\text{in garnet}}{2/3Mg_3Al_2Si_3O_{12}} + \underset{\text{quartz}}{SiO_2} \quad (11)$$

$$\underset{\text{in orthopyroxene}}{Mg_2Si_2O_6} + \underset{\text{in orthopyroxene}}{MgAl_2SiO_6} \rightleftharpoons \underset{\text{in garnet}}{Mg_3Al_2Si_3O_{12}} \quad (12)$$

Anorthite activity in plagioclase was estimated by the Al-avoidance model of Perkins and Newton (1981). For MG-20, a visual estimate of the proportions of An_{50} and An_{35} plagioclase was made to estimate a weighted average of An_{45}. Diopside and enstatite activities are derived from data of Wood and Banno (1973). Interaction parameters were used to estimate pyrope and grossular activity in garnet according to Perkins and Newton (1981).

Geobarometers based on (10) and (11) have recently been calibrated by Perkins and Newton (1981); results from mafic gneiss of the Kapuskasing Zone are presented in Table 4. Wood (1977) applied Equilibrium (8) to granulites as a geobarometer. Using a calibration of (8) based on thermochemical data of Helgeson *et al.* (1978), pressure estimates are seen to be controlled mainly by the formulation of the $CaAl_2SiO_6$ activity model. Wood's (1978) formulation leads to a cluster of values in the 4 kbar range whereas Wood's (1979) model produces results averaging ~15 kbar. Equilibria (9) and (12) are subject to the same uncertainty.

Wood's (1974) calibration of (12) gives additional pressure estimates for garnet, orthopyroxene-bearing assemblages. Pressure was estimated for a Gt–Sl–Pl–Bt–Qz assemblage according to Ghent's (1976) calibration.

The accuracy of the various geobarometers is limited by the uncertainty in probe analyses, greatest where accurate analyses of small quantities of alumina in pyroxene are required ((8), (9), (12)). The low dP/dT slope of (10) and (11) and their use of major components recommend these equilibria as reliable geobarometers.

Pressure estimates

Estimates of peak metamorphic pressure depend on the assumption that present mineral compositions are not significantly different than those at the peak metamorphic conditions. In samples with retrograde amphibole, this assumption may not be valid because other minerals, including plagioclase, could have changed their compositions during retrograde reactions, presumably at lower P,T. Such reactions could also have occurred in response to changes in a_{H_2O} at peak P,T.

The Perkins and Newton (1981) calibration of (10) yields pressure values generally in the range 5.4–8.4 kbar, averaging 6.3 kbar. The results are plotted on Figure 9 along with values derived from (11) and (12). The average pressure for the area from (11) is 7.7 kbar and individual values are commonly ~2 kbar higher than those estimated from (10) for the same or proximal samples. Values from (10) are generally lower than those from (11), either because of different blocking temperatures in different mineral systems or uncertainty in the thermodynamic calibration (Newton and Perkins, 1982). A 6.3 kbar reference line separates areas with above-average apparent values from those with lower values. The line includes a roughly north–south-trending area of relatively high apparent pressure in the central and eastern Kapuskasing Zone (Fig. 9). This pattern supports the preliminary interpretation (Percival, 1981a) that the Kapuskasing Zone is at the base of a tilted, west-dipping crustal section. However, diffusion considerations may preclude this simple interpretation (see below).

Assuming that pressure is a function of depth, approximately 20–25 km of overburden has been eroded from the Kapuskasing zone. Previous estimates of relative uplift of

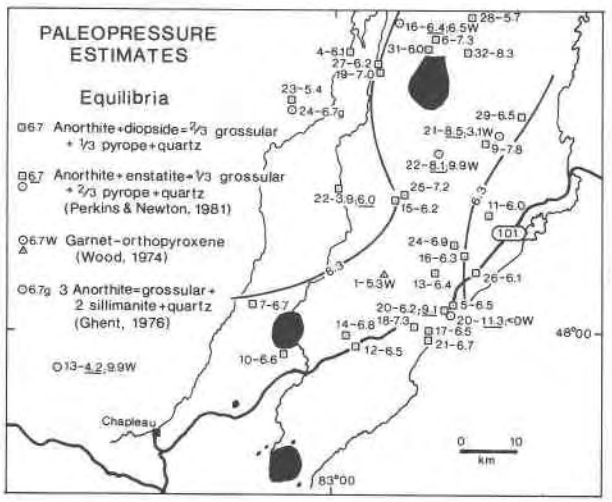

Fig. 9. Paleopressure map of part of the Chapleau–Foleyet area. Symbols represent rock type (circles: PG-series; squares: MG-series; triangles: OG-series), keyed in to sample identifier (numbers to left of dash). Numbers to the right of the dash are pressure estimates, in kbar, keyed in to the equilibrium used to derive the value. The 6.3 kbar reference line is based on the anorthite–diopside–grossular–pyrope–quartz equilibrium.

the Kapuskasing Zone with respect to adjacent regions where 8 km, based on heat-flow data (Cermak and Jessop, 1971) and at least several thousand feet (Thurston *et al.*, 1977). Pressure-sensitive assemblages are lacking in the terranes to the east and west. However, slate some 5 km east of the Ivanhoe Lake cataclastic zone is at relatively low grade (chlorite–muscovite). Although dP/dT is generally not constant with depth (P. H. Thompson, 1977), assuming an average crustal geothermal gradient of ~30°C/km, biotite should form at the expense of muscovite–chlorite at about 450°C, corresponding to a depth of about 15 km. Therefore, relative uplift along the Ivanhoe Lake cataclastic zone is estimated to be at least 5 and possibly greater than 10 km, based on metamorphic considerations.

Water activity calculations

Water activity was calculated for rocks containing assemblages corresponding to Mg end-member dehydration equilibria for which *P–T* estimates were available. Three equilibria have been used for this purpose, including (2):

$$\underset{\text{in hornblende}}{Ca_2Mg_5Si_2O_{22}(OH)_2} \rightleftharpoons \underset{\text{in orthopyroxene}}{3MgSiO_3} + \underset{\text{in clinopyroxene}}{2CaMgSi_2O_6} + \underset{\text{quartz}}{SiO_2} \quad (13)$$

$$\underset{\text{in biotite}}{KMg_3AlSi_3O_{10}(OH)_2} + \underset{\text{quartz}}{3SiO_2} \rightleftharpoons \underset{\text{in orthopyroxene}}{3MgSiO_3} + \underset{\text{in K-feldspar}}{KAlSi_3O_8} + H_2O \quad (14)$$

Relation (15) was solved for f_{H_2O}:

$$\Delta G^\circ = -RT \ln K - \Delta V_s(P - 1) \quad (15)$$

Activity of solids were estimated by ideal ionic solution models and thermochemical data are from Helgeson *et al.* (1978) and Haselton and Westrum (1980). Water activity is calculated as f_{H_2O} as defined by (15), divided by f_{H_2O} of pure water at P,T as defined by Helgeson and Kirkham (1974). Derived values are found in Tables 2, 4 and 6.

Equilibrium (13) yields values <0.1; (14) gives results <0.4 and (2) yields some values above 1.0. Values in excess of 1.0 indicate that the minerals were not in equilibrium at the specified *P–T* conditions. For example, brown hornblende in MG-11 yields $a_{H_2O} = 0.853$ whereas actinolite, presumed to be of retrograde origin, yields a mechanically-unsustainable value of 5.5. Green, secondary amphiboles indicate higher a_{H_2O} in every example (*e.g.*, MG-4, 11, 20), but would yield lower a_{H_2O} values if a lower temperature were assumed.

No pattern of regional variation in water activity is obvious from values plotted on a map. Values are generally on the order of 0.1 near the western edge of the Kapuskasing Zone but do not show a regional trend for the rest of the area. There is no correlation between calculated water activity and the presence or absence of orthopyroxene. The estimates are in the range of values reported for granulite-facies terranes (*e.g.*, Bohlen and Essene (1976b) for the Adirondacks; Horrocks (1980) for the Limpopo Belt) and for the Broken Hill area of Australia (Phillips, 1980).

Significance of pressure–temperature results

A comparison between *P–T* estimates for individual samples and probable *P–T* conditions in the Gt–Cpx–Pl and orthopyroxene zones shows that temperature estimates for rocks containing orthopyroxene are below the Gt–Cpx zone conditions deduced by mineral-melt equilibria. Eight of twenty-five estimates from the Gt–Cpx–Pl zone fall within the Gt–Cpx zone on the *P–T* diagram; the rest fall below. This pattern suggests that Fe–Mg exchange between mineral pairs continued during cooling and that derived temperature estimates are somewhat retrograde.

For the Conemarra region, Yardley (1977) suggested that temperature above 640°C had homogenized prograde zonation in garnets by intragranular diffusion. Lasaga *et al.* (1977) estimated that retrograde Fe–Mg exchange between the outer 10–15 μm of adjacent garnet and cordierite grains occurred down to ~450°C. In view of the quenching problem it may be realistic to regard the highest apparent temperatures, in the 800°C range, as closest to peak temperature. The lower values probably record quenching at later times. By this reasoning, the pressure and temperature estimates, based on mineral

systems with probable different blocking temperatures (O'Hara, 1977), may not even record a *P–T* condition through which the rock passed. Thus it is hazardous to attempt to deduce either a prograde or cooling metamorphic path for the area, based on geothermobarometry.

"High-pressure granulites"

The assemblage almandine garnet–clinopyroxene–plagioclase–quartz is diagnostic of the regional hypersthene zone according to Winkler (1979, p. 260, 267–268). de Waard (1965) and Green and Ringwood (1967) suggested that this assemblage forms as an alternative to orthopyroxene–plagioclase during high-pressure granulite-facies metamorphism. Turner (1981) attaches a different significance to the assemblage, regarding it as transitional from amphibolite to granulite facies based on Binns' (1964) study. In the present study area, the location of the Gt–Cpx–Pl zone between Hb–Pl±Cpx rocks and orthopyroxene-bearing rocks suggests that it characterizes the amphibolite–granulite facies transition. Although the assemblage is the same as that in the Adirondacks (de Waard, 1965) and temperature conditions were similar (Bohlen and Essene, 1977), the path of metamorphism was different. In the Grenville Province, the development of garnet–clinopyroxene assemblages has been attributed to isobaric cooling of orthopyroxene–plagioclase granulites (Martingole and Schrijver, 1971; Whitney, 1978) whereas in the Kapuskasing Zone, garnet and clinopyroxene formed during prograde reactions.

Conclusions

In the eastern Wawa subprovince and Kapuskasing Structural Zone, three metamorphic zones are defined on the basis of assemblages in mafic rocks. The sequence Hb–Pl, Cpx–Hb–Pl, Gt–Cpx–Pl suggests easterly-increasing grade. Both hornblende- and biotite-bearing rocks in four areas surrounded by the Gt–Cpx–Pl zone contain metamorphic orthopyroxene, representing the highest grade attained. Tonalitic melt is thought to have been responsible for reducing a_{H_2O} in the metamorphic fluid in mafic gneiss to values of 0.5–0.7 at temperatures of ~750°C, at which point Hb–Pl began to produce Gt–Cpx-melt assemblages by vapour-absent melting reactions. Biotite in adjacent migmatitic paragneiss units was stable at these conditions but began to break down to orthopyroxene–K-feldspar-melt by vapour-absent-melting reactions at ~770°C, a_{H_2O} ~0.5. Orthopyroxene first appears in mafic rocks at similar conditions.

Estimates of metamorphic pressure and temperature by various calibrations are 3.1–9.9 kbar, 600–825°C but most values are between 6.0 and 7.3 kbar and 650 and 775°C. The orthopyroxene-zone rocks yield average to below-average values suggesting that the peak-metamorphic distribution of elements has been altered, probably by ionic diffusion during cooling.

Acknowledgments

This paper represents part of the writer's Ph.D. thesis at Queen's University. The guidance and encouragement of Drs. D. M. Carmichael and H. Helmstaedt and research funds provided through their NSERC grants are gratefully acknowledged. A special debt of gratitude is owed to D. M. Carmichael for use of computer programs and for patience as a tutor in thermodynamics. Field work was supported by the Geological Survey of Canada, through Dr. K. D. Card, who suggested the project and provided continuous encouragement. Field assistance was enthusiastically undertaken by J. B. Percival and R. Valenta. Discussions with the above, as well as Drs. K. Coe, T. E. Krogh and L. Riccio were invaluable in the development of ideas presented here. The manuscript in various forms has received the benefit of critical comments from K. D. Card, D. M. Carmichael, H. Helmstaedt, R. C. Newton, M. Schau, M. R. St-Onge, P. H. Thompson and especially E. Froese. Financial support in the form of NSERC and OGS scholarships to the writer are gratefully acknowledged.

References

Allen, J. C., Boettcher, A. L., and Marland, G. (1975) Amphiboles in andesite and basalt: I. Stability as a function of *P–T–*fO_2. American Mineralogist, 60, 1069–1085.

Amit, O. and Eyal, Y. (1976) The genesis of Wadi Magrish migmatites (N–E Sinai). Contributions to Mineralogy and Petrology, 59, 95–110.

Ashworth, J. A. (1976) Petrogenesis of migmatites in the Huntly–Portsoy area, northeast Scotland. Mineralogical Magazine, 40, 661–682.

Arth, J. G. and Hanson, G. N. (1972) Quartz diorites derived by partial melting of eclogite or amphibolite at mantle depths. Contributions to Mineralogy and Petrology, 37, 161–174.

Bence, A. E. and Albee, A. L. (1968) Empirical correction factors for the electron microanalysis of silicates and oxides. Journal of Geology, 76, 382–403.

Bennett, G., Brown, D. D., George, P. T., and Leahy, E. J. (1967) Operation Kapuskasing. Ontario Department of Mines Miscellaneous Paper 10.

Binns, R. A. (1964) Zones of progressive regional metamorphism in the Willyama complex, Broken Hill District, New South Wales. Journal of the Geological Society of Australia, 11, 283–330.

Bishop, F. C. (1980) The distribution of Fe^{2+} and Mg between coexisting ilmenite and pyroxene with applications to geothermometry. American Journal of Science, 280, 46–77.

Bohlen, S. R. and Essene, E. J. (1977) Feldspar and oxide thermometry of granulites in the Adirondack Highlands. Contributions to Mineralogy and Petrology, 62, 153–169.

Bohlen, S. R. and Essene, E. J. (1978) Igneous pyroxenes from metamorphosed anorthosite massifs. Contributions to Mineralogy and Petrology, 65, 433–442.

Bohlen, S. R. and Essene, E. J. (1979a) A critical evaluation of two-pyroxene thermometry in Adirondack granulites. Lithos, 12, 335–345.

Bohlen, S. R. and Essene, E. J. (1979b) Calculations of water activities in biotite-sillimanite gneisses throughout the Adirondacks. Geological Society of America Program with Abstracts, 11, 39.

Bohlen, S. R. and Essene, E. J. (1980) Evaluation of coexisting

garnet–biotite, garnet–clinopyroxene, and other Fe–Mg exchange thermometers in Adirondack granulites: Summary. Geological Society of America Bulletin, 91, 107–109.

Brown, G. C. and Fyfe, W. S. (1970) The production of granitic melts during ultrametamorphism. Contributions to Mineralogy and Petrology, 28, 310–318.

Buddington, A. F. (1963) Isograds and the role of H_2O in metamorphic facies of orthogneisses from the northwest Adirondack area, New York. Geological Society of America Bulletin, 74, 1155–1183.

Buddington, A. F. and Lindsley, D. H. (1964) Iron–titanium oxides and synthetic equivalents. Journal of Petrology, 5, 310–357.

Cermak, V. and Jessop, A. (1971) Heat flow, heat generation and crustal temperatures in the Kapuskasing area of the Canadian Shield. Tectonophysics, 11, 287–303.

Chinner, G. A. (1960) Pelitic gneisses with varying ferrous/ferric ratios from Glen Cova, Angus, Scotland. Journal of Petrology, 1, 178–217.

Clemens, J. D. and Wall, V. J. (1981) Origin and crystallization of some peraluminous (S-type) granitic magmas. Canadian Mineralogist, 19, 111–131.

de Waard, D. (1965) The occurrence of garnet in granulite-facies terrain of the Adirondack Highlands. Journal of Petrology, 6, 165–191.

Deer, W. A., Howie, R. A., and Zussman, J. (1966) An Introduction to the Rock-forming Minerals. Longman, London.

Eggler, D. H. (1972) Amphibole stability in H_2O-undersaturated calc-alkaline melts. Earth and Planetary Science Letters, 15, 28–34.

Ellis, D. J. and Green, D. H. (1979) An experimental study of the effect of Ca upon garnet–clinopyroxene Fe–Mg exchange equilibria. Contributions to Mineralogy and Petrology, 71, 13–22.

Ferry, J. M. (1980) A comparative study of geothermometers and geobarometers in pelitic schists from south-central Maine. American Mineralogist, 65, 720–732.

Ferry, J. M. and Spear, F. S. (1978) Experimental calibration of the partitioning of Fe and Mg between biotite and garnet. Contributions to Mineralogy and Petrology, 66, 113–117.

Friend, C. R. L. (1981) Charnockite and granite formation and influx of CO_2 at Kabbaldurga. Nature, 294, 550–552.

Ganguly, J. (1979) Garnet and clinopyroxene solid solutions, and geothermometry based on Fe–Mg distribution coefficient. Geochimica et Cosmochimica Acta, 43, 1021–1029.

Ghent, E. D. (1976) Plagioclase–garnet–Al_2SiO_5–quartz: a potential geobarometer–geothermometer. American Mineralogist, 61, 710–714.

Ghent, E. D., Robbins, B., and Stout, M. Z. (1979) Geothermometry, geobarometry and fluid compositions of metamorphosed calc-silicates and pelites, Mica Creek, British Columbia. American Mineralogist, 64, 874–885.

Goldsmith, J. R. and Newton, R. C. (1977) Scapolite–plagioclase stability relations at high pressures and temperatures in the system $NaAlSi_3O_8$–$CaAl_2Si_2O_8$–$CaCO_3$–$CaSO_4$. American Mineralogist; 62, 1063–1081.

Goodwin, A. M. (1965) Geology of Heenan, Marion, and northern Genoa Townships, district of Sudbury. Ontario Department of Mines Geological Report 38.

Goodwin, A. M. (1977) Archean basin–craton complexes and the growth of Precambrian shields. Canadian Journal of Earth Sciences, 14, 2737–2759.

Gower, C. F., Paul, D. K., and Crocket, J. H. (1982) Protoliths and petrogenesis of Archean gneisses from the Kenora area, English River subprovince, northwest Ontario. Precambrian Research, 17, 245–274.

Green, D. H. and Ringwood, A. E. (1967) An experimental investigation of the gabbro to eclogite transformation and its petrological applications. Geochimica et Cosmochimica Acta, 31, 763–833.

Hansen, B. (1981) The transition from pyroxene granulite facies to garnet clinopyroxene granulite facies. Experiments in the system CaO–MgO–Al_2O_3–SiO_2. Contributions to Mineralogy and Petrology, 76, 234–242.

Haselton, H. T. and Westrum, E. F. (1980) Low-temperature heat capacities of synthetic pyrope, grossular, and $pyrope_{60}$ $grossular_{40}$. Geochimica et Comochimica Acta, 44, 701–709.

Helgeson, H. C. and Kirkham, D. H. (1974) Theoretical prediction of the thermodynamic behaviour of aqueous electrolytes at high pressures and temperatures: I. Summary of the thermodynamic/electrostatic properties of the solvent. American Journal of Science, 274, 1089–1198.

Helgeson, H. C., Delany, J. M., Nesbitt, H. W., and Bird, D. K. (1978) Summary and critique of the thermodynamic properties of rock-forming minerals. American Journal of Science 278A.

Helz, R. T. (1976) Phase relations of basalts in their melting ranges at P_{H_2O} = 5 kb: Part II, Melt composition. Journal of Petrology, 17, 139–193.

Holloway, J. R. and Burnham, C. W. (1972) Melting relations of basalt with equilibrium water pressure less than total pressure. Journal of Petrology, 13, 1–29.

Horrocks, P. C. (1980) Ancient Archaean supracrustal rocks from the Limpopo mobile belt. Nature, 286, 596–599.

Innes, M. J. S. (1960) Gravity and isostasy in northern Ontario and Manitoba. Dominion Observatory Ottawa Publication, 21, 263–338.

Janardhan, A. S., Newton, R. C., and Hansen, E. C. (1982) The transformation of amphibolite facies gneiss to charnockite in southern Karnataka and northern Tamil Nadu, India. Contributions to Mineralogy and Petrology, 79, 130–149.

Kilinc, I. A. (1979) Melting relations in the quartz diorite–H_2O and quartz diorite–H_2O–CO_2 systems. Neues Jahrbuch für Mineralogie Monatshefte, 62–72.

Kretz, R. (1982) Transfer and exchange equilibria in a portion of the pyroxene quadrilateral as deduced from natural and experimental data. Geochimica et Cosmochimica Acta, 46, 411–421.

Krogh, T. E. and Turek, A. (1982) Precise U–Pb zircon ages from the Gamitagama greenstone belt, southern Superior Province. Canadian Journal of Earth Sciences, 19, 859–867.

Krogh, T. E., Davis, D. W., Nunes, P. D., and Korfu, F. (1982) Archean evolution from precise U–Pb isotopic dating, Geological Association of Canada Abstracts with Program, 7, 61.

Lal, R. K. and Moorehouse, W. W. (1969) Cordierite–gedrite rocks and associated gneisses of Fishtail Lake, Harcourt Township, Ontario. Canadian Journal of Earth Sciences, 6, 145–165.

Lasaga, A., Richardson, S. M., and Holland, H. D. (1977) The mathematics of cation diffusion and exchange between silicate minerals during retrograde metamorphism. In S. K. Saxena and S. Bhattacharji, Eds., Energetics of Geological Processes, p. 353–388. Springer-Verlag, Berlin, Heidelberg, New York.

MacLaren, A. S., Anderson, D. T., Fortescue, J. A. C., Gaucher, E. G., Hornbrook, E. H. W. , and Skinner, R. (1968)

A preliminary study of the Moose River Belt, northern Ontario. Geological Survey of Canada Paper 67–38.

Martingole, J. and Schrijver, K. (1971) Association of (hornblende) garnet–clinopyroxene "subfacies" of metamorphism and anorthosite masses. Canadian Journal of Earth Sciences, 8, 698–704.

Newton, R. C. and Perkins, D. III (1982) Thermodynamic calibration of geobarometers based on the assemblages garnet–plagioclase–orthopyroxene(clinopyroxene)–quartz. American Mineralogist, 67, 203–222.

Nunes, P. D. and Pyke, D. R. (1980) Geochronology of the Abitibi metavolcanic belt, Timmins–Matachewan area-progress report. In E. G. Pye, Ed., Summary of Geochronology Studies 1977–1979, p. 34–39. Ontario Geological Survey Miscellaneous Paper 92.

O'Hara, M. J. (1977) Thermal history of excavation of Archaean gneisses from the base of the continental crust. Journal of the Geological Society of London, 134, 185–200.

Parsons, G. E. (1961) Niobium-bearing complexes east of Lake Superior. Ontario Department of Mines Geological Report 3.

Percival, J. A. (1981a) Stratigraphic, structural and metamorphic relations between the Wawa and Abitibi subprovinces and the Kapuskasing Structural Zone near Chapleau, Ontario. In Card, K. D., Percival, J. A., Lafleur, J. and Hogarth, D. D., Progress report on regional geological synthesis, central Superior Province, p. 83–90. Current Research, Part A, Geological Survey of Canada, Paper 81–1A.

Percival, J. A. (1981b) Geology of the Kapuskasing Structural Zone in the Chapleau–Foleyet area, Geological Survey of Canada Open File Map 763.

Percival, J. A. and Coe, K. (1981) Parallel evolution of Archaean low- and high-grade terrane: a view based on relationships between the Abitibi, Wawa and Kapuskasing belts. Precambrian Research, 14, 315–331.

Percival, J. A. and Krogh, T. E. (1983) U–Pb zircon geochronology of the Kapuskasing structural zone and vicinity in the Chapleau–Foleyet area, Ontario. Canadian Journal of Earth Sciences, 20, 830–843.

Percival, J. A., Loveridge, W. D., and Sullivan, R. W. (1981) U–Pb zircon ages of tonalitic metaconglomerate cobbles and quartz monzonite from the Kapuskasing Structural Zone in the Chapleau area, Ontario. In Rb–Sr and U–Pb Isotopic Age Studies, Report 4. Current Research, Part C, Geological Survey of Canada Paper 81-1C, 107–113.

Perkins, D. III and Newton, R. C. (1981) Charnockite geobarometers based on coexisting garnet–pyroxene–plagioclase–quartz. Nature, 292, 144–146.

Phillips, G. N. (1980) Water activity changes across an amphibolite–granulite facies transition, Broken Hill, Australia. Contributions to Mineralogy and Petrology, 75, 377–386.

Powell, R. (1978) The thermodynamics of pyroxene geotherms. Philosophical Transactions of the Royal Society of London A 288, 457–469.

Raheim, A. and Green, D. H. (1974) Experimental determination of the temperature and pressure dependence of the Fe–Mg partition coefficient for coexisting garnet and clinopyroxene. Contributions to Mineralogy and Petrology, 48, 179–203.

Raheim, A. and Green, D. H. (1975) *P,T* paths of natural eclogites during metamorphism—a record of subduction. Lithos, 8, 317–328.

Reinhardt, E. W. (1968) Phase relations in cordierite-bearing gneisses from the Gananoque area, Ontario. Canadian Journal of Earth Sciences, 5, 455–482.

Ribbe, P. H. (1975) Exsolution textures and interference colors in feldspars. In P. H. Ribbe, Ed., Feldspar Mineralogy, R73–96. Mineralogical Association of America Short Course Notes, Vol. 2. Washington, D.C.

Riccio, L. (1981) Geology of the northeastern portion of the Shawmere anorthosite complex, district of Sudbury. Ontario Geological Survey Open File Report 5338.

Robertson, J. A. and Wyllie, P. J. (1971) Rock–water systems, with special reference to the water deficient region. American Journal of Science, 271, 252–277.

Roeder, P. L., Campbell, I. H., and Jamieson, H. E. (1979) A re-evaluation of the olivine–spinel geothermometer. Contributions to Mineralogy and Petrology, 68, 325–334.

Ross, M. and Huebner, J. S. (1975) A pyroxene geothermometer based on composition-temperature relationships of naturally occurring orthopyroxene, pigeonite and augite. International Conference on Geothermometry and Geobarometry Pennsylvania State University (extended abstract).

Saxena, S. K. (1979) Garnet–clinopyroxene geothermometer. Contributions to Mineralogy and Petrology, 70, 229–235.

Stockwell, C. H. (1979) Geology of the Canadian Shield–introduction. In R. J. W. Douglas, Ed., Geology and Economic Minerals of Canada, p. 44–54. Geological Survey of Canada, Economic Geology Report 1 (5th edition).

Stormer, J. C. Jr. (1975) A practical two-feldspar geothermometer. American Mineralogist, 60, 667–674.

Stout, J. H. (1972) Phase petrology and mineral chemistry of coexisting amphiboles from Telemark, Norway. Journal of Petrology, 13, 99–145.

Streckeisen, A. (1976) To each plutonic rock its proper name. Earth Science Reviews, 12, 1–33.

Thompson, P. H. (1977) Metamorphic *P–T* distributions and geothermal gradients calculated from geophysical data. Geology, 5, 520–522.

Thurston, P. C., Siragusa, G. M., and Sage, R. P. (1977) Geology of the Chapleau area, districts of Algoma, Sudbury and Cochrane. Ontario Division of Mines Geoscience Report 157.

Turek, A., Smith, P. E., and Van Schmus, W. R. (1982) Rb–S and U–Pb ages of volcanism and granite emplacement in the Michipicoten belt–Wawa, Ontario. Canadian Journal of Earth Sciences, 19, 1608–1626.

Turner, F. J. (1981) Metamorphic Petrology: Mineralogical, Field and Tectonic Aspects, second edition. McGraw-Hill, New York.

Weaver, B. L. (1980) Rare-earth geochemistry of Madras granulites. Contributions to Mineralogy and Petrology, 71, 271–279.

Wells, P. R. A. (1977) Pyroxene thermometry in simple and complex systems. Contributions to Mineralogy and Petrology, 62, 129–139.

Wells, P. R. A. (1979) Chemical and thermal evolution of Archaean sialic crust, southern West Greenland. Journal of Petrology, 20, 187–226.

Wendlandt, R. F. (1981) Influence of CO_2 on melting of model granulite facies assemblages: a model for the genesis of charnockites. American Mineralogist, 66, 1164–1174.

Whitney, P. R. (1978) The significance of garnet "isograds" in granulite facies rocks of the Adirondacks. In: Metamorphism in the Canadian Shield. Geological Survey of Canada Paper 78-10, 357–366.

Winkler, H. G. F. (1979) Petrogenesis of Metamorphic Rocks, 5th ed. Springer-Verlag, Berlin, Heidelburg, New York.

Wood, B. J. (1974) The solubility of alumina in orthopyroxene coexisting with garnet. Contributions to Mineralogy and Petrology, 46, 1–15.

Wood, B. J. (1977) The activities of components in clinopyroxene and garnet solid solutions and their application to rocks. Philosophical Transactions of the Royal Society of London, A 286, 331–342.

Wood, B. J. (1978) Reactions involving anorthite and $CaAl_2SiO_6$ pyroxene at high pressures and temperatures. American Journal of Science, 278, 930–942.

Wood, B. J. (1979) Activity-composition relationships in $Ca(Mg,Fe)Si_2O_6$–$CaAl_2SiO_6$ clinopyroxene solid solutions. American Journal of Science, 279, 854–875.

Wood, B. J. and Banno, S. (1973) Garnet–orthopyroxene and orthopyroxene–clinopyroxene relationships in simple and complex systems. Contributions to Mineralogy and Petrology, 42, 109–124.

Yardley, B. W. D. (1977) An empirical study of diffusion in garnet. American Mineralogist, 62, 793–800.

Yoder, H. S. Jr. (1967) Albite–anorthite–quartz–water at 5 kb. Carnegie Institution of Washington Year Book, 66, 477–478.

Manuscript received, May 4, 1982;
accepted for publication, February 3, 1983.